2012

Flexibility and Transient Dynamic Analysis of a Slider-Crank Deployment Mechanism

Andres Cavezza
West Virginia University

Flexibility and Transient Dynamic Analysis of a Slider-Crank Deployment Mechanism

Andres Cavezza

Thesis Submitted to the
Benjamin M. Statler College of Engineering and Mineral Resources
at West Virginia University
in partial fulfillment of the requirements
for the degree of

Master of Science
in
Mechanical Engineering

Victor Mucino, Ph.D., Chair
Mridul Gautam, Ph.D.
Wade W. Huebsch, Ph.D.
Kenneth H. Means, Ph.D.

Department of Mechanical Engineering

Morgantown, West Virginia

2012

Keywords: High Speed Deployment Mechanism; Flexibility; Transient Analysis; Dynamic Analysis; Slider - Crank

ABSTRACT

Flexibility and Transient Dynamic Analysis of a

Slider-Crank Deployment Mechanism

by

Andres Cavezza

Master of Science in Mechanical Engineering

West Virginia University

High Speed Deployment Mechanisms (HSDM) have become essential and indispensable for specific applications in industrial and aerospace sectors. However, the field of High Speed Deployment Mechanisms is still not completely explored in many areas; the holistic analysis of HSDM reveals a lack of information about its, classification, analysis and design considerations. A research was conducted to generate a systematic approach addressing the issues mentioned above. In the beginning of this research, a methodology is presented to perform the kinematic and dynamic analyses of a Slider-Crank Deployment Mechanism; this method is based on the Lagrange Multipliers approach. The analyses of position, velocity, acceleration and reaction forces were carried out obtaining reliable results. In addition, the results were validated with the implementation of commercial software (ANSYS^{TM}, ABAQUS^{TM} and SOLIDWORKS^{TM}). Moreover, structural, transient and modal finite element analyses were developed for components of the mechanism to study stresses, strains, deformations and natural frequencies. Also, an illustrative aerospace application and a CAD model were proposed for the studied mechanism. Finally, an important contribution in the literature of HSDM was made: a criterion to verify if the assumption of using rigid bodies in a Slider-Crank Deployment Mechanism can be adopted.

Dedicated To My Parents

Antonio & Ma Elena

And Brother

Vicenzo

ACKNOWLEDGEMENTS

I acknowledge the help and guidance I received from my research advisor and committee chair **Dr. Victor H. Mucino**. I am grateful that he has been not only a great advisor but also a friend in the last few years. Furthermore, I am deeply grateful that he gave me the opportunity to collaborate in his program “Industrial Outreach Program in Mexico” during the last 4 years. All the experiences which we have faced together in Queretaro, Mexico and Morgantown, U.S.A have helped to develop and improve my professional and personal qualities.

I also would like to express my gratitude to Dr. Mridul Gautam, Dr. Wade W. Huebsch and Dr. Kenneth H. Means for serving in committee and providing support throughout my research.

I am deeply grateful to Florence Spiegel, Alex Sanchez, Karen Flores de Jesus and Jerry Wong from West Virginia University for their help and support during my research.

TABLE OF CONTENTS

LIST OF FIGURES

LIST OF TABLES

NOMENCLATURE

M	*Degree of freedom or mobility.*
L	*Number of links.*
J_1	*Number of 1 DOF joints.*
J_2	*Number of 2 DOF joints.*
γ	*Mobility parameter.*
j	*Total number of kinematic constraints.*
f_i	*Connectivity of the i^{th} joint.*
$q_1, q_2, \dots q_n$	*Generalized Coordinates.*
Ψ^k	*Kinematic constraints.*
Ψ^D	*Driving constraints.*
$[\Psi_q]$	*Jacobian Matrix.*
$\{\gamma\}$	*Gamma vector.*
$\{\Psi_t\}$	*Vector of partial derivative of the constraint equation*
$\{\Psi_{tt}\}$	*Vector of the second partial derivative of the constraint equation.*
λ	*Vector of Lagrange multipliers.*
$\ddot{q}$	*Vector of generalized accelerations.*
T	*Represents the kinetic energy.*
V	*Potential energy.*
L	*Lagrangian function.*
L^*	*Objective function.*
$\{\ddot{q}\}$	*Vector of accelerations.*
$\{\lambda\}$	*Lagrange multipliers vector.*
$[M]$	*Mass matrix.*
$\{F_e\}$	*Generalized forces vector.*
m^i	*Mass of the body i.*
${I_G}^i$	*Mass moment of inertia defined with respect to the center of mass of the body.*
nb	*Number of bodies.*
m_{cr}	*Mass of crank*
I_{cr}	*Inertia of the crank*
m_{co}	*Mass of the connecting road.*
I_{co}	*Inertial of the connecting road.*
m_{sl}	*Mass of the slider.*
I_{sl}	*Inertial of the slider.*
T	*Natural Period*
n	*Number of times that the T is smaller the deployment time ($\Delta t = 0.016128s$).*
k	*Times that the natural period is less that the deployment time.*

Chapter 1

INTRODUCTION

1.1 BACKGROUND

High Speed Deployment Mechanisms (HSDM) have a wide range of applications in mechanical and aerospace systems. Research centers of space technology play an important role in the development of new technologies for this type of mechanisms. Because of the advantages of high speed deployment mechanisms, a high percentage of space machines are based on those kinds of mechanisms. For example, satellites, space structures, space transportation systems and more. Such space machines or structures are subjected to extreme operating conditions. Different mechanical elements such as links, joints, actuators, springs dampers, etc. are directly affected by those conditions. As a result, dynamic and kinematic analyses need to be considered in the development and the improvement of a design methodology of high speed deployment mechanisms.

High speed deployment mechanisms are also used in the military industry in order to increase the performance of a variety of specific machines, mainly in ballistic applications. When HSDM are used in ballistic application, extreme boundary conditions and loads are presented in systems which increase the complexity in design and

dynamic analyses. To name an example, a hybrid projectile which needs to be launched and to deploy its wings in the air using a high speed deployment mechanism. This mechanism is subjected to different loads and conditions such as high accelerations, air resistance, friction force and different pressures during the explosion process. Consequently, a special methodology needs to be applied in the design, the kinematic and the dynamic analyses of HSDM. It allows creating reliable, safe and accurate mechanisms with a high precision in different extreme operating conditions.

Nowadays, the industry plays an important role in our daily life; we are depending on industrial developments and products to satisfy needs. As a result, companies need to be competitive and capable of development to affect the market. Consequently, manufacturing processes need to be increased and improved to meet the demands of the global competition. Among others, the implementation of high speed deployment mechanisms in industries has shown to be a reasonable solution to manufacturing process; especially in sectors such as automobile, aerospace, textile, and mining industry. Furthermore, those mechanisms have responded to the current demands of customers such as high performance, reliability, precision and durability.

High speed deployment mechanisms are implemented in a system to accomplish a specific task; this process asks for many design considerations to gain a reliable result. Essential information such as loads and boundary conditions need to be analyzed and considered for the design. In addition, clearance and contact between components which are interconnecting in a system with other elements need to be analyzed and developed. That leads to some important questions in the design scenario; how can the

HSDM be identified from non HSDM? How the kinematic and dynamic analyses can be performed in HSDM? Can rigid bodies be used in HSDM?

How the mechanical components or links of the HSDM mechanisms can be affected with high accelerations?

Many classifications of mechanisms are already known; based on different parameters. For instance, the number of degrees of freedom, functionality, theories, number of links or bars and others. However, when high speed deployment mechanisms are analyzed, there is not a lot of information found in the literature about their classification, design and dynamic analysis. For this reason, the classification, design and analysis of these types of mechanisms are potential areas of research in the present and near future.

1.2 PROBLEM STATEMENT

High speed deployment mechanisms have become essential and indispensable for specific machines, structures and mechanical devices in space technology, industrial applications and aerospace industry. However, the holistic analysis of high speed deployment mechanisms reveals a lack of information about its, classification, analysis and design. A classification of high speed deployment mechanisms has not been found in the literature review; no systematic approach or nomenclature has been made to classify and analyze these mechanisms. The creation of a nomenclature or systematic approach for studying high speed deployment mechanisms would generate a general

chart to analyze HSDM. Consequently, the main characteristics, properties, advantages, disadvantages, differences and similarities of HSDM can be recognized.

In addition, the literature survey has shown that the methodology in designing high speed deployment mechanisms has not been properly documented either. That is because a clear and precise theory of design which includes all related considerations, theories and issues has not been developed yet. Contact, clearance and friction in joints and elements are factors which affect the design of high speed deployment mechanisms. Therefore, dynamic and kinematic analyses need to be included in design considerations.

In conclusion, the kinematic and dynamic analyses of a Slider-Crank Deployment Mechanism will be developed in this research. In addition, the results from those analyses will be validated with the implementation of commercial software. Finally, a criterion to establish the use of rigid or flexible body assumption in a Slider-Crank Deployment Mechanism will be proposed.

1.3 OBJECTIVE OF THESIS

The objective of this research is to develop an approach to analyze a Slider-Crank Deployment Mechanism to study the flexibility and dynamic transient response in the mechanism. In this research, emphasis is made on the importance of generating a methodology or a general approach as a reference point in the literature of HSDM. Essential topics need to be addressed in this research such as i) Applications of high

speed deployment mechanisms ii) Dynamics and kinematics analyses of HSDM iii) Design considerations of a Slider-Crank Deployment Mechanism iv) The study of rigid or flexible bodies in a Slider-Crank Deployment Mechanism. Furthermore, the connection and correlation among these issues will be explained in this thesis.

1.4 SCOPE OF THESIS

In this research thesis, a Slider-Crank Deployment Mechanism will be studied and analyzed in order to establish a reference frame in the scientific literature. This study addresses the topic from different points of view to develop a clear and better understanding of high speed deployment mechanisms. Furthermore, a variety of analyses will be carried out to perform the studies of HSDM; equations, techniques and theories from the literature review will be used in the calculations. Additionally, some effective commercial programs are implemented to simulate models, such as ANSYS™, ABAQUS™, MATLAB™ and SOLID WORKS™.

Chapter 2

LITERATURE REVIEW

2.1 INTRODUCTION

The mechanical behavior and dynamic analysis of high speed deployment mechanisms are essential topics which need to be addressed in the design process. The reliability of a system may be affected when these types of mechanisms are subjected to extreme loads such as high velocity and acceleration. Nowadays, high performance in machinery and structures is a requirement in the global market which increases significantly the complexity of design of multibody systems.

The literature survey has showed that design considerations for high speed deployment mechanisms have not been strongly addressed yet. No methodology about how to analyze and to design high speed deployment mechanism has been found in the technical literature. The Mechanical Engineering perspective of a design process can be defined as a problem solving process; based on a specific problem a solution concept is created which will carry out a final product [1].

A mechanism is a device which transmits motion to a predetermined set of outputs or paths. Today, through the rapid development of industry, and increased requirements for products on the global market mechanisms are the vital element of a machine; they are essential in mechanical engineering. A variety of different mechanisms are used in a wide range of applications in industrial areas such as automotive, aerospace, manufacturing, mining, and others. [2].

2.3 AEROSPACE APPLICATIONS

Some researchers have developed different analyses of deployment mechanisms for aerospace applications. However, analyses of high speed deployment mechanism were not found in the literature. Pankow et al. in [3] developed a research which addresses the design and on-orbit deployment for a mechanism in a fast satellite, but they only considered small deployment velocities in their research. Rossoni et al. in [4] studied a deployment mechanism for the space technology 5 micro satellite; this design has been tested and qualified for flight. Kerhousse et al. in [5] presented a research about a deployment mechanism for a deployable radiator for the French national space agency; this research was focused on the mechanism and the actuator design. Wallrapp and Wiedemann in [6] developed a study of a flexible solar array for small velocity of deployment.

Similarly, there are other projects for aerospace applications which involve nanotechnology. Sangree et al. in [25] presented a study about deployment mechanisms for a nanosatellite. In this research an original idea was developed how two separate small satellites from each other. It focused on the dynamic analysis of rotation, acceleration and translation of the deployed components in a microgravity environment. In 2010, Sapna et al. in [26] published a study about a controlled deployment mechanism for space applications. In this research, the implementation of inflatable booms was necessary to deploy the sunshield in the mechanism. Finally, design, analyses and testing of a space inflatable structure were carried out by this study. In 2010, Olivier and Falcke in [27] from the Radbound University in Holland presented a study for a deployment mechanism of an antenna. The design of a

deployment mechanism was presented and some finite element analyses were set up. Furthermore, this work also presents the selection of materials and an explanation about the electronic system of the antenna model. Murata et al. in [28] conducted a research about a deployable antenna for space application. In this study the dimension of the satellite was restricted; the new design had to be small enough to fit properly into the room of the launcher. This issue represented a challenging situation for designing the deployable mechanism for the antenna.

2.4 CRYOGENIC, BALLISTIC AND INDUSTRIAL APPLICATIONS

Deployment mechanisms have also been implemented in cryogenic, ballistic and industrial applications. Strom et al. in [7] proposed a design and an analysis method for the nozzle deployment mechanism for the Vinci Cryogenic Engine. This project was developed for Snecma Space Engine Division in Vernon, France. Condon and Hollis in [13] performed dynamic analyses for a mortar dragster tab mechanism. In this study, a rigid body simulation was carried out to analyze some specific parts of a mortar. Narayana et al. in [8] presented a simulation of a deployable polyhedral truss for a large antenna. This mechanism has 18 bays which form an 18 sided polygon. This research implemented the commercial software ADAMS for some analyses.

2.5 KINEMATIC AND DYNAMIC ANALYSES

The kinematic and dynamic analyses of mechanisms have been studied for many years by researches. Nevertheless, these analyses have not been focused on high speed deployment mechanisms. Osman and Dukkipati in [9] presented an algebraic approach to determine the velocity fluctuation in spatial four link mechanisms.

Ranjbarkohan et al. in [10] studied the kinematic and kinetic analysis of a slider-crank mechanism for a four cylinder Z24 engine. In this paper the problem was analyzed with high loads in the system such as maximum values of engine power and maximum torque. Flores in [11] proposed a dynamic analysis of a system with imperfect kinematic joints. In this study, Flores focused on the influence of imperfect kinematic joints in multibody systems. In 2006, Koshy in [12], from the Wichita State University, presented a dissertation in which a mechanical system was analyzed with real joints. Koshy studied in his work important topics such as clearance and impact in joints in flexible bodies.

2.6 CLERANCE AND CONTACT EFFECTS IN MECHANISMS

A lot of researchers have focused on other important issues in mechanisms such as clearance effects, contact, impact and design of joints for different applications. In 2002, Bauchau in [14] studied the clearance effects for revolute and spherical joints for a flexible multibody system. Important topics were addressed such as clearance, lubrication and friction phenomena by Bauchau. Moreover, a dynamic analysis was developed for a nonlinear system. Schwab et al. in [15] proposed a study in which clearance in revolute joints for rigid and elastic systems was analyzed. In addition, the research studied how clearance in revolute joints affects the dynamic response of mechanisms or machines. In 2012, Haround and Megahed in [29] presented an interesting research about the clearance in revolute joints for a slider - crank mechanism. This paper compared the experimental and the simulation results of the clearance for one revolute joint of the mechanism. The simulation part was developed by different software applications for dynamic simulations. The results between the two

approaches obtained in this paper were coherent and reasonable. Consequently, the new approach presented by Haround and Megahed seems to be acceptable and reliable. This approach consists of modeling the mechanism with a dry clearance joints.

The contact in joints is a fundamental issue which needs to be addressed. Raman in [16] presented some applications of the Hert'z theory of impact; this work shows different equations to calculate the impact in a specific system. Furthermore, experimental data was compared to carry out some important observations about the Hertz's theory. Fu in [17] proposed a study for the Hertz's theory of contact mechanics in which axisymmetric normal contact between 2 elastics bodies was analyzed. Besides that, Fu explained a procedure to handle this type of difficulty. Finally, a contact model between a sphere and a cone was presented and analyzed.

Similarly, Earles and Seneviratne in [18] presented a study which described and analyzed contact losses in a revolute joint. In this research the Authors modeled the joint clearances by the implementation of additional degrees of freedom in the system. Finally, they worked out equations of motion for this system, and they determined an expression of the force magnitude of the clearance. In 1983, Hamilton in [19] showed a formula to analyze the stress in a sliding spherical contact. The Hertz's theory and the Minlin were implemented in this study to develop some passages for establishing boundary conditions. Moreover, Hamilton also considered friction effects on the system in his work.

2.7 TRIBOLOGY

In addition to joint analyses, studies of lubrication play an important role in the joint design. Some significant researches concerning this topic have been found in the literature review, and will be outlined in the following paragraph.

In 1983, Booker in [20] studied the effects of a lubricant which was subjected to variable loads. Moreover, the dynamic behavior of a bearing was analyzed by implementing different approaches. Lee et al. in [21] presented an optimization analysis for a journal bearing under refrigerant applications. In this project many parameters such as friction, clearance and lubrication effects were taken into consideration. A mathematical model and a computer program were set up to solve the problem. In the end, the effect of changing the original design was found, and a comparison was made between old and new models. In [22] Dowson et al. studied a bearing which was used for biomechanics application; lubrication and contact have been considered in this work. The literature survey showed some considerable studies concerning tribology for different applications, but no analyses for high speed deployment mechanisms.

2.8 IMPACT LOADS

In some applications mechanisms are subjected to impact loads which affect directly the behavior of joints and other components; as for example in ballistic applications. Some joints are designed to resist such impact loads and to maintain a high performance. In 2004, MA et al. in [23] presented an analysis of joints for ballistics applications. The study presented a model run by a commercial software to simulate and to analyze the behavior of joints under impact. Finally, MA et al. suggested an

optimized design for joints which supports the impact load. Another dissertation was carried out by Nakalswamy in [24] in which a structure with joints was subjected to impact loads. This work presented experimental and numerical analysis of the model; the finite element method was implemented in the research. Furthermore, a transient analysis was performed to run some model simulations, and the shock propagation was also taken in consideration.

Chapter 3

Methodology

This research presents a general approach to establish a methodology to perform the analysis of a High Speed Deployment Mechanism. This mechanism consists of a slider - crank mechanism in which the slider is interconnected by a helical spring between two bodies. To carry out a successful design of such a mechanism, many studies need to be developed. The dynamic and kinematic analyses of a mechanism are essential in the study of HSDM. In addition to those analyses, design considerations for different components of the system must be performed; for example, the design of actuators such as springs or cams. This study analyzes the issues mentioned above, and presents a methodology to develop an analysis for a Slider-Crank mechanism.

In the first part of this research, a kinematic analysis (Chapter 4) is performed for the slider - crank mechanism. The topological analysis was developed by following the Gruebler's and Kutzbach's approaches. Then, the analytical and mathematical procedures are proposed to establish the constraint equations of the system. Finally, the analysis ends up with systems of equations for solving the position, velocity and acceleration for the mechanism. For solving these systems of equations, a multibody program needed to be implemented in the commercial software Matlab ^{TM}. This program is a modification of a software code developed by the University of Rome Tor Vergata,

and was provided by PhD student Lorenzo Mariti. This code takes and processes the information of the constraint equations and the input data such as geometry, topology and initial conditions of the mechanism. Finally, a Matlab function called “fsolve’’ was applied to solve the system.

In Chapter 5, a dynamic analysis is described for a Slider-Crank Deployment Mechanism. The theoretical dynamic analysis of the mechanism is performed with the use of the Lagrange Multipliers method. With this method it is possible to define a new objective function which can be treated as a function of other variables; it facilitates the solution process of the system. Then, the stationary conditions for the Lagrange function are established. After that, the Lagrange equation needs to be modified for constrained systems to perform the dynamic analysis of the slider - crank mechanism. This modification can be made by the implementation of the Hamiltonian formulation for a constrained optimization problem. With the use of this technique the new objective function is the Hamilton integral. This integral can be expressed in terms of the generalized coordinates and constraint equations obtained in the kinematic analysis. Finally, it is possible to end up with a differential algebraic system of equations which contains the same number of unknowns and number of equations. The implementation of a multi body code developed in the commercial software Matlab was needed to solve the differential algebraic system of equations. This code is a modification of the original program developed by the University of Rome Tor Vergata which was provided by PhD student Lorenzo Mariti. In the Matlab program the solver ODE was used to compute the necessary calculations for solving the problem; the position, velocity and acceleration of the system were obtained. Furthermore, the reaction forces at joints were calculated.

In Chapter 6, finite elements analyses and design considerations are addressed for some components of the slider-crank mechanism. First, a slider-crank model is built in the commercial software SolidWorks^{TM}. Then, by using the study motion of SolidWorks^{TM} the position, velocity and acceleration analyses are performed. In addition to those calculations, the reaction forces at joints are calculated as well. Second, the spring which interconnects the slider of the mechanism is examined with a finite element method. A dynamic explicit analysis is set up in the commercial software ABAQUS^{TM} to analyze stresses and deformations of the spring under loads. Finally, modal and transient analyses are presented in the commercial software ANSYS^{TM} to establish a criterion about the use of rigid or flexible bodies in HSDM.

Based on the result from the analyses and calculations mentioned above, some contributions will be proposed in the literature of High Speed Deployment Mechanism.

Chapter 4

Kinematic Analysis

A kinematic analysis of a mechanism is defined as an analysis which studies the motion of the bodies without regarding to forces. A kinematic analysis will be developed for the high speed deployment mechanism. The high speed deployment mechanism has a slider crank configuration and is connected by a spring in the slider.

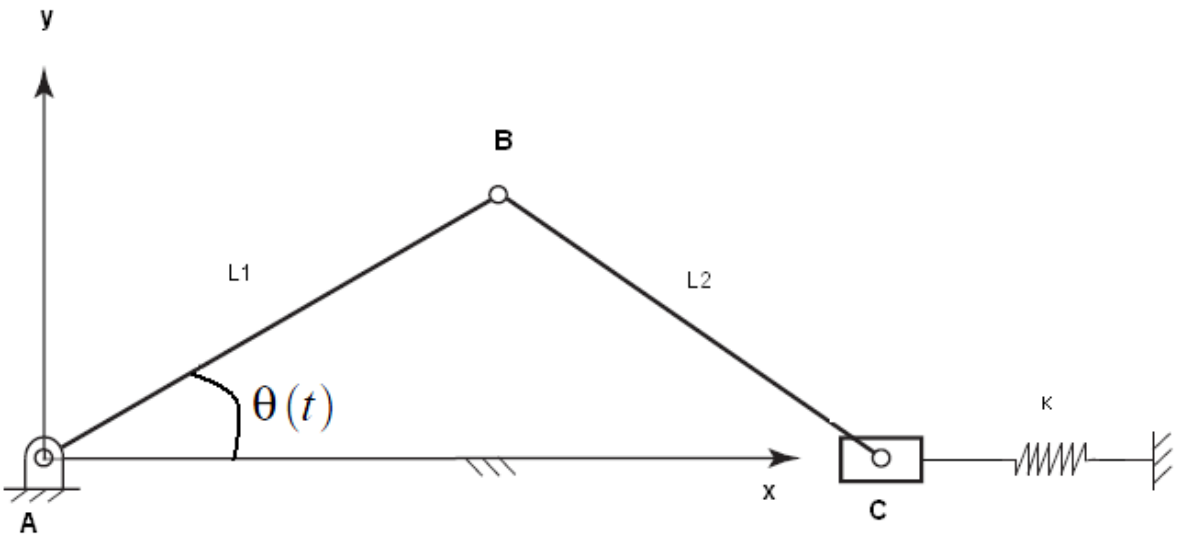

Figure 1 Slider- Crank mechanism

L_1 and L_2 are the crank and the coupler lengths respectively. L_1 = 0.040 m and L_2 = 0.080m.The spring constant is defined by k = 1500N/m. The frame, crank, coupler and slider are interconnected with revolute joints. The data was taken from a study developed in collaboration with Lorenzo Mariti et al. [32]

4.1 TOPOLOGICAL ANALYSIS

The number of degree of freedom for this mechanism can be determined by the Gruebler's equation in Norton [2].

$$M = 3(L-1) - 2J_1 - J_2 \qquad \text{Eq. 1}$$

Where

- ✓ M = degree of freedom or mobility.
- ✓ L = number of bodies (including the frame)
- ✓ J_1 = number of 1 DOF joints.
- ✓ J_2 = number of 2 DOF joints.

Substituting into Eq.1

$$M = 3\,(4\text{-}1) - 2\,(4) = 1$$

The number of degree of freedom can also be computed by using the Kutzbach's equation

$$M = \gamma\,(L - j - 1) + \sum_{i=1}^{j} f_1 \qquad \text{Eq. 2}$$

- ✓ γ = Mobility parameter.
- ✓ j = Total number of kinematic constraints.
- ✓ f_i = Connectivity of the i^{th} joint.

Substituting into Eq. 2

$$F = 3\,(4 - 4 - 1) + 4 = 1$$

The system shown in the figure has one degree of freedom.

4.2 PLANAR KINEMATIC CONSTRAINT EQUATIONS

4.2.1 GENERALIZED COORDINATES

In order to establish the joint constraints in a mechanism, kinematic relationships need to be developed. These relationships are expressed by algebraic equations which contain the coordinates of the different elements of the system.

The generalized coordinates (GC) are defined as a set of variables which specifies the position and the orientation of all the bodies in the system. A local reference frame needs to be defined in each body in order to establish the configuration of the system. The number of generalized coordinates is defined by

$$nc = 3\ x\ nb \qquad \text{Eq. 3}$$

- ✓ nc = number of generalized coordinates
- ✓ nb = number of bodies
- ✓

From Eq. 3

$$nc = 3\ x\ 3 = 9$$

The mechanism has 9 generalized coordinates. The generalized coordinates are shown in the figure.

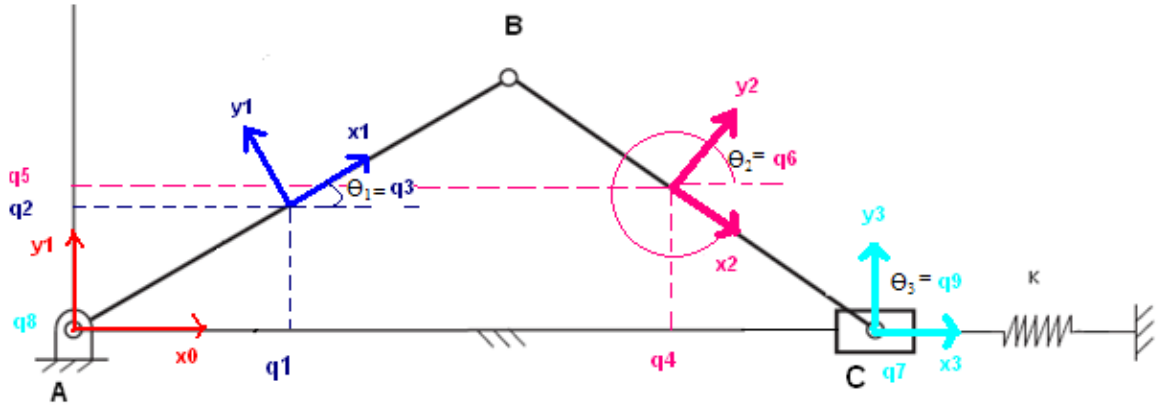

Figure 2 Generalized Coordinates

The vector of the generalized coordinates is defined by

$$\{q\} = \begin{Bmatrix} q_1 \\ q_2 \\ q_3 \\ q_4 \\ q_5 \\ q_6 \\ q_7 \\ q_8 \\ q_9 \end{Bmatrix} \quad \text{Eq. 4}$$

Where the generalized coordinates are defined as

$$q_1 = \frac{L_1}{2}\cos\theta_1 \quad \text{Eq. 5}$$

$$q_2 = \frac{L_1}{2}\sin\theta_1 \quad \text{Eq. 6}$$

$$q_3 = \theta_1 \quad \text{Eq. 7}$$

$$q_4 = L_1\cos\theta_1 + \frac{L_2}{2}\cos\theta_2 \quad \text{Eq. 8}$$

$$q_5 = -\frac{L_2}{2}\sin\theta_2 \quad \text{Eq. 9}$$

$$q_6 = \theta_2 \quad \text{Eq.10}$$

$$q_7 = \frac{L_1}{2}\cos\theta_1 + \frac{L_2}{2}\cos\theta_2 \quad \text{Eq.11}$$

$q_8 = 0$ Eq. 12

$q_9 = 0$ Eq. 13

4.2.2 CONSTRAINT EQUATION SYSTEM

If a kinematic constraint is imposed between 2 bodies, the relative motion of the bodies is defined by certain conditions. Furthermore, these conditions could be expressed in algebraic equations in terms of generalized coordinates; these algebraic equations are also known as holonomic kinematic constraint equations. Besides, there are other kinematic constraints which are time dependent, those are known as rehonomic or driving constraints.

The analyzed mechanism presents 8 holonomic kinematic constraint equations which do not explicitly depend on time and can be expressed as

$$\{\Psi^k(\{q\})\} = \left\{\Psi_1^k, \Psi_2^k, \Psi_3^k, \Psi_4^k, \Psi_5^k, \Psi_6^k, \Psi_7^k, \Psi_8^k\right\}^T = 0 \quad \text{Eq.14}$$

The mechanism does not have rehonomic or driving constraints $\{\Psi^D(\{q\}, t)\}$ because there are not time depending kinematic couplings.

Finally, the constraint equation system is given by

$$\begin{Bmatrix} \{\Psi^k(\{q\}\} \\ \{\Psi^D(\{q\}, t\} \end{Bmatrix} = 0 \quad \text{Eq. 15}$$

4.2.3 CONSTRAINT EQUATIONS FOR THE REVOLUTE JOINT

The slider crank mechanism has 3 revolute joints; but only one relative rotation is allowed between the bodies which are connected by revolute joints. For example, the point B (see figure 2) in the slider crank mechanism belongs to the crank and coupler

link, so using the constraint equation for a revolute joint it is possible to impose the coincidence between the points. The same approach is used to establish the coincidence between point A and C.

The kinematic constraint equations for point A are given by

$$\Psi_{1,2} = \begin{Bmatrix} q_1 - \frac{L_1}{2}\cos q_3 \\ q_2 - \frac{L_1}{2}\sin q_3 \end{Bmatrix} = 0 \qquad \text{Eq. 16}$$

The kinematic constraint equations for the point B are given by

$$\Psi_{3,4} = \begin{Bmatrix} q_1 + \frac{L_1}{2}\cos q_3 - q_4 + \frac{L_2}{2}\cos q_6 \\ q_2 + \frac{L_1}{2}\sin q_3 - q_5 + \frac{L_2}{2} sin q_6 \end{Bmatrix} = 0 \qquad \text{Eq. 17}$$

The kinematic constraint equations for the point C are given by

$$\Psi_{5,6} = \begin{Bmatrix} q_4 + \frac{L_2}{2}\cos q_6 - q_7 \\ q_5 + \frac{L_2}{2}\sin q_6 - q_8 \end{Bmatrix} = 0 \qquad \text{Eq. 18}$$

4.2.4 CONSTRAINT EQUATIONS FOR THE PRISMATIC JOINT

The constraint equations for a translational joint establish the relative translation between 2 bodies which is the only motion that is allowed for a prismatic joint.

In order to determine Ψ_8 it is necessary to set up three points in two different bodies. The points D_i, E_i and F_j are shown in the figure 3. Furthermore, the angles of the local reference frame with respect to the global reference frame need to be defined (q_i, q_f).

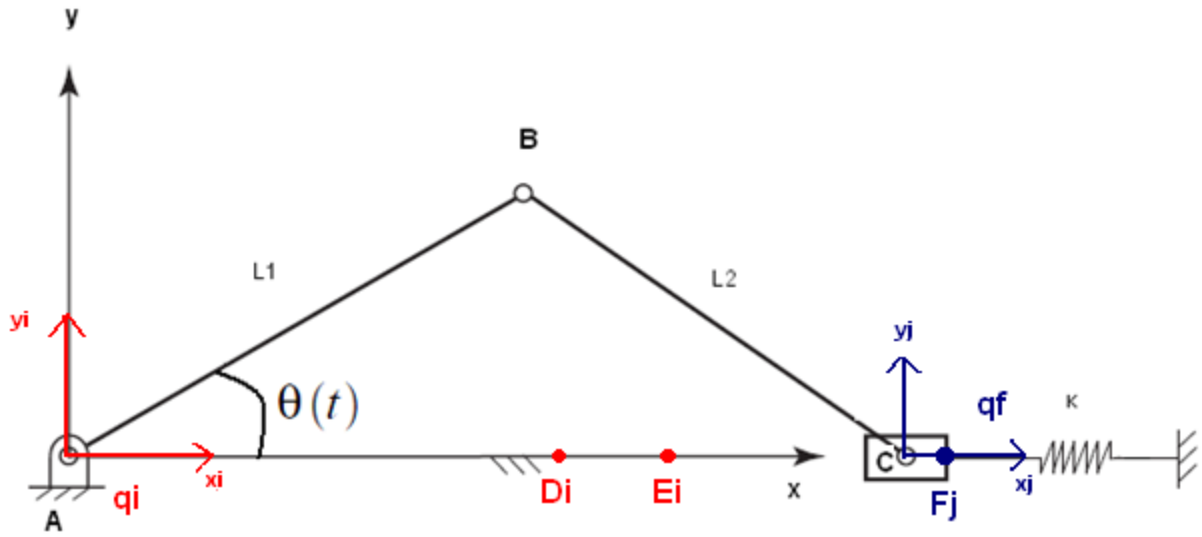

Figure 3 Constrain Equations for the prismatic joint

The angle

$$\begin{vmatrix} 0_{X_{D_i}} & 0_{X_{D_j}} & 1 \\ 0_{X_{E_i}} & 0_{X_{E_j}} & 1 \\ 0_{X_{F_i}} & 0_{X_{F_j}} & 1 \end{vmatrix} = \Psi_7 = 0 \qquad \text{Eq. 19}$$

The angle Ψ_7 is given from Eq. 19 by

$$\Psi_7 = 0 \qquad \text{Eq. 20}$$

Ψ_8 $c$an be determined by the next relationship

$$\Psi_8 = q_i - q_j - \Delta\Phi_{ij} = 0 \qquad \text{Eq. 21}$$

Since there is not a relative rotation between bodies i and j the angle $\Delta\Phi_{ij}$ has to be constant. By substituting the values in the equation above presented

$$\Psi_8 = 0 \qquad \text{Eq. 22}$$

4.2.5 KINEMATIC CONSTRAINT VECTOR

Combining the kinematic and driving constraints equations it is possible to end up with:

$$\{\Psi(\{q\},t)\} = \begin{Bmatrix} q_1 - \frac{L_1}{2}\cos q_3 \\ q_2 - \frac{L_1}{2}\sin q_3 \\ q_1 + \frac{L_1}{2}\cos q_3 - q_4 + \frac{L_2}{2}\cos q_6 \\ q_2 + \frac{L_1}{2}\sin q_3 - q_5 + \frac{L_2}{2} sin q_6 \\ q_4 + \frac{L_2}{2}\cos q_6 - q_7 \\ q_5 + \frac{L_2}{2}\sin q_6 - q_8 \\ q_8 \\ q_9 \end{Bmatrix} \qquad \text{Eq. 23}$$

4.2.6 VELOCITY AND ACCELERATION ANALYSIS

In order to compute the velocity and the acceleration analysis it is necessary to calculate the Jacobian Matrix $[\Psi_q]$, gamma vector $\{\gamma\}$, and the first and the second partial derivatives with respect to time of the constraint vector $\{\Psi_t\}$ and $\{\Psi_{tt}\}$ respectively.

The Jacobian Matrix for the system can be calculated by taking the partial derivatives of the vector function

$$[\Psi_q] = \frac{\partial\{\Psi\}}{\partial\{q\}} \qquad \text{Eq. 24}$$

$$[\Psi_q] = \begin{bmatrix} 1 & 0 & \frac{L_1}{2}\sin q_3 & 0 & 0 & 0 & 0 & 0 & 0 \\ 0 & 1 & -\frac{L_1}{2}\cos q_3 & 0 & 0 & 0 & 0 & 0 & 0 \\ 1 & 0 & -\frac{L_1}{2}\sin q_3 & -1 & 0 & -\frac{L_2}{2}\sin q_6 & 0 & 0 & 0 \\ 0 & 1 & \frac{L_1}{2}\cos q_3 & 0 & -1 & \frac{L_2}{2}\cos q_6 & 0 & 0 & 0 \\ 0 & 0 & 0 & 1 & 0 & -\frac{L_2}{2}\cos q_6 & -1 & 0 & 0 \\ 0 & 0 & 0 & 0 & 1 & \frac{L_2}{2}\cos q_6 & 0 & -1 & 0 \\ 0 & 0 & 0 & 0 & 0 & 0 & 0 & 1 & 0 \\ 0 & 0 & 0 & 0 & 0 & 0 & 0 & 0 & 1 \end{bmatrix} \quad \text{Eq. 25}$$

The velocity vector is given by

$$\{\dot{q}\} = \begin{Bmatrix} \dot{q}_1 \\ \dot{q}_2 \\ \dot{q}_3 \\ \dot{q}_4 \\ \dot{q}_5 \\ \dot{q}_6 \\ \dot{q}_7 \\ \dot{q}_8 \\ \dot{q}_9 \end{Bmatrix} \quad \text{Eq. 26}$$

The vector of partial derivative with respect to time of the constraint equation is defined as

$$\{\Psi_t\} = \left\{\frac{\partial \Psi}{\partial t}\right\} \quad \text{Eq. 27}$$

$$\{\Psi_t\} = \begin{Bmatrix} 0 \\ 0 \\ 0 \\ 0 \\ 0 \\ 0 \\ 0 \\ 0 \end{Bmatrix} \quad \text{Eq. 28}$$

The vector of the second partial derivative with respect to time of the constraint equation is defined as

$$\{\Psi_{tt}\} = \left\{\frac{\partial^2 \Psi}{\partial t^2}\right\} \quad \text{Eq. 29}$$

$$\{\Psi_{tt}\} = \begin{Bmatrix} 0 \\ 0 \\ 0 \\ 0 \\ 0 \\ 0 \\ 0 \\ 0 \end{Bmatrix} \quad \text{Eq. 30}$$

The gamma vector is expressed with the following relationship

$$\{\gamma\} = -\left(\left[\Psi_q\right]\{\dot{q}\}\right)_q \{\dot{q}\} - 2\left\{\Psi_{tq}\right\}\{\dot{q}\} - \{\Psi_{tt}\} \quad \text{Eq. 31}$$

Substituting the values in Eq. 31

$$\{\gamma\} = \begin{Bmatrix} -\frac{L_1}{2}\dot{q_3}^2 \cos q_3 \\ -\frac{L_1}{2}\dot{q_3}^2 \sin q_3 \\ \frac{L_1}{2}\dot{q_3}^2 \cos q_3 + \frac{L_2}{2}\dot{q_6}^2 \cos q_6 \\ \frac{L_1}{2}\dot{q_3}^2 \sin q_3 + \frac{L_2}{2}\dot{q_6}^2 \sin q_6 \\ \frac{L_2}{2}\dot{q_6}^2 \cos q_6 \\ \frac{L_2}{2}\dot{q_6}^2 \sin q_6 \\ 0 \\ 0 \end{Bmatrix} \quad \text{Eq. 32}$$

Finally, the velocity and the acceleration analyses are expressed by the following systems of equations:

Velocity Analysis

$$[\Psi_q]\{\dot{q}\} = \{\Psi_t\} \quad \text{Eq. 33}$$

Acceleration Analysis

$$[\Psi_q]\{\ddot{q}\} = \{\gamma\} \quad \text{Eq. 34}$$

4.3 KINEMATIC ANALYSIS IN MATLAB

A Matlab code was written in order to compute the kinematic analysis of the slider-crank mechanism. The code follows the methodology presented in the previous chapter 4.2

4.3.1 POSITION ANALYSIS IN MATLAB

The following graph shows the behavior of the slider in 1 second.

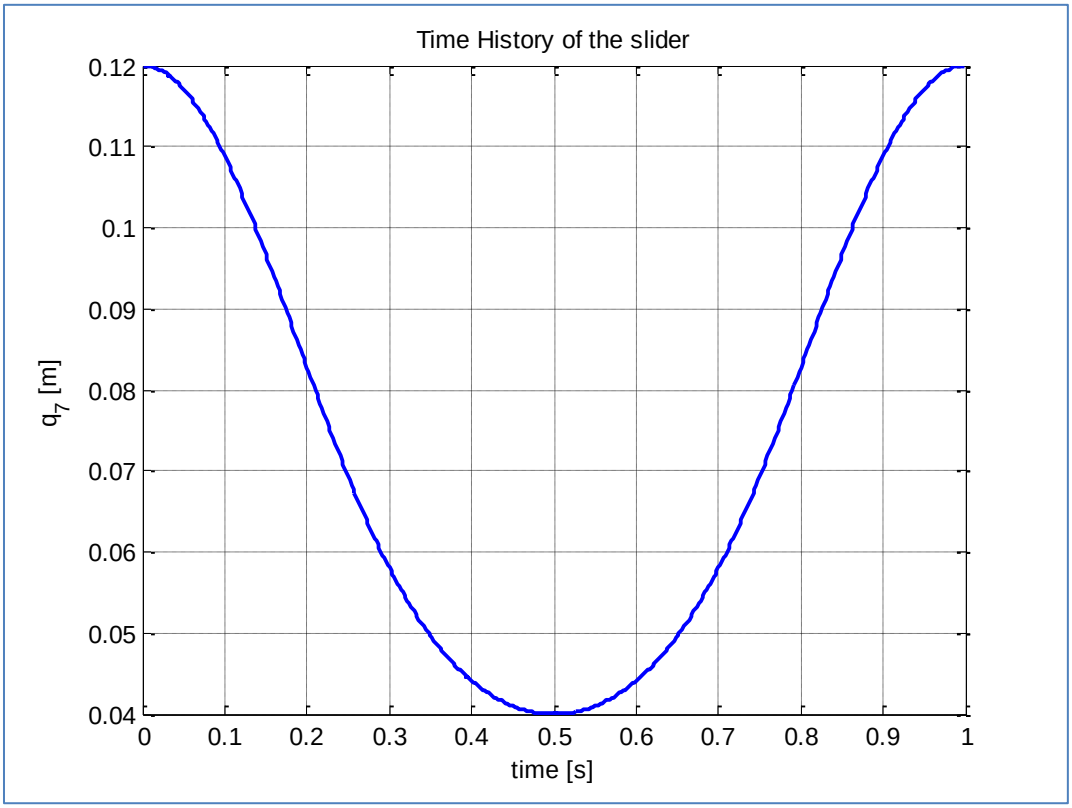

Figure 4 Time vs. Position of the Slider in Matlab

The total displacement 80 mm is reached at 0.5s.

4.3.2 VELOCITY ANALYSIS IN MATLAB

The velocities for the slider are shown in the following graph

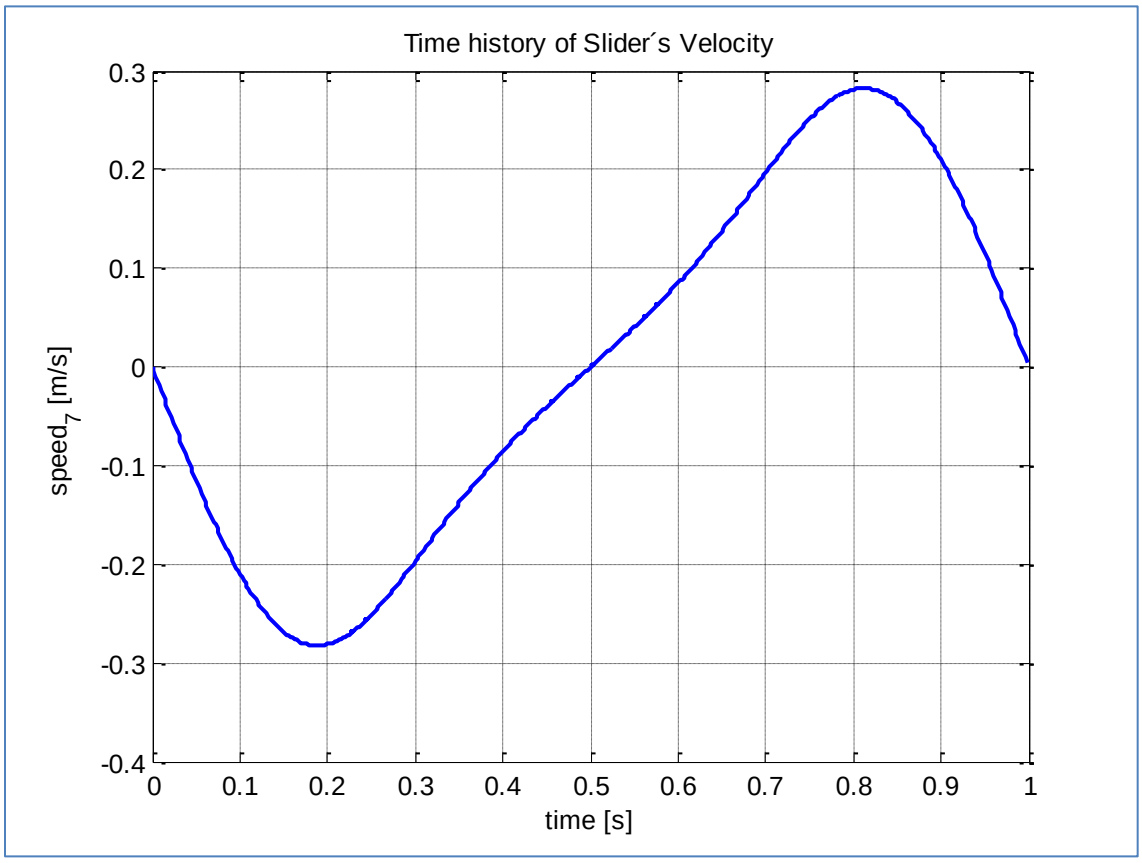

Figure 5 Time vs. velocity of the slider in Matlab

The graph shows that the maximum velocity is 0.28 m/s and the minimum is - 0.28 m/s.

4.3.3 ACCELERATION ANALYSIS IN MATLAB

The acceleration analysis was performed in Matlab and the results are shown in the figure 6.

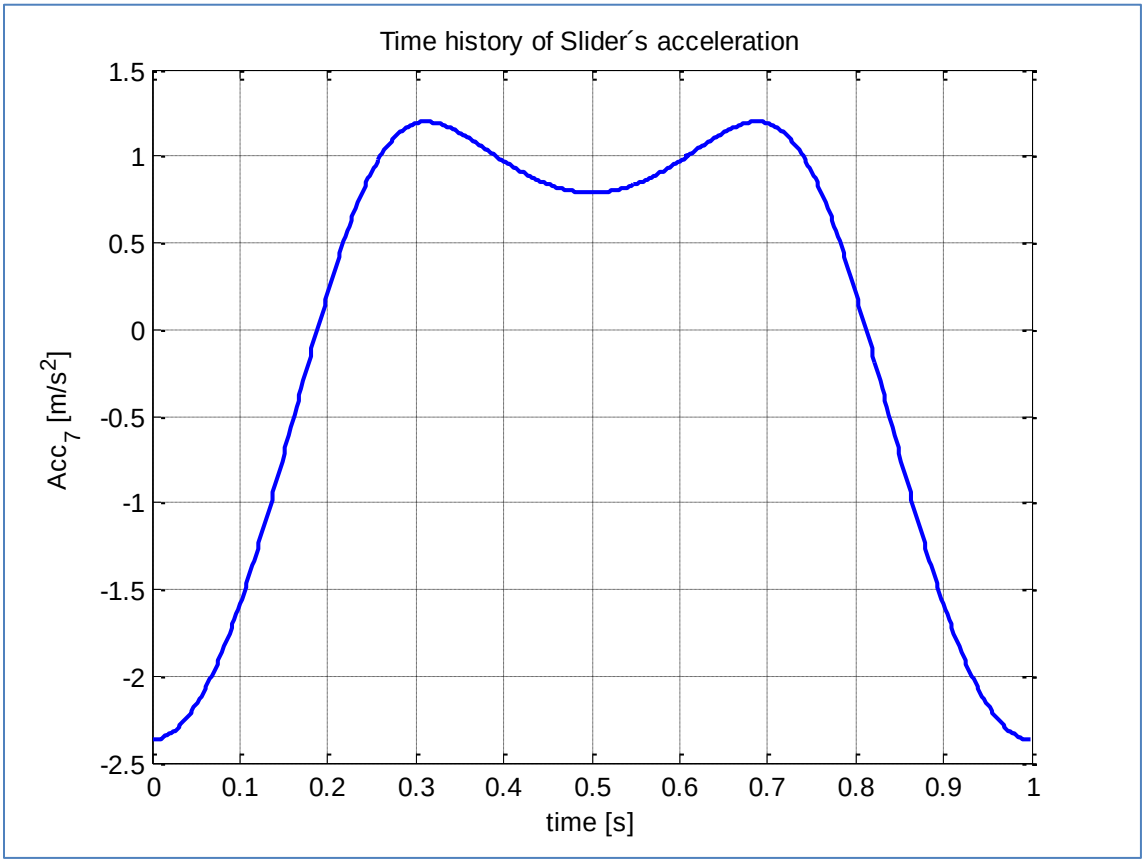

Figure 6 Time vs. Acceleration of the Slider in Matlab

The maximum value of the acceleration is 1.2 m/s^2 and the minimum is – 2.3 m/s^2.

Finally, in order to verify the results from Matlab it is necessary to trace the trajectory of the midpoint on the crank. The trajectory should describe a circle as it is shown in the next figure

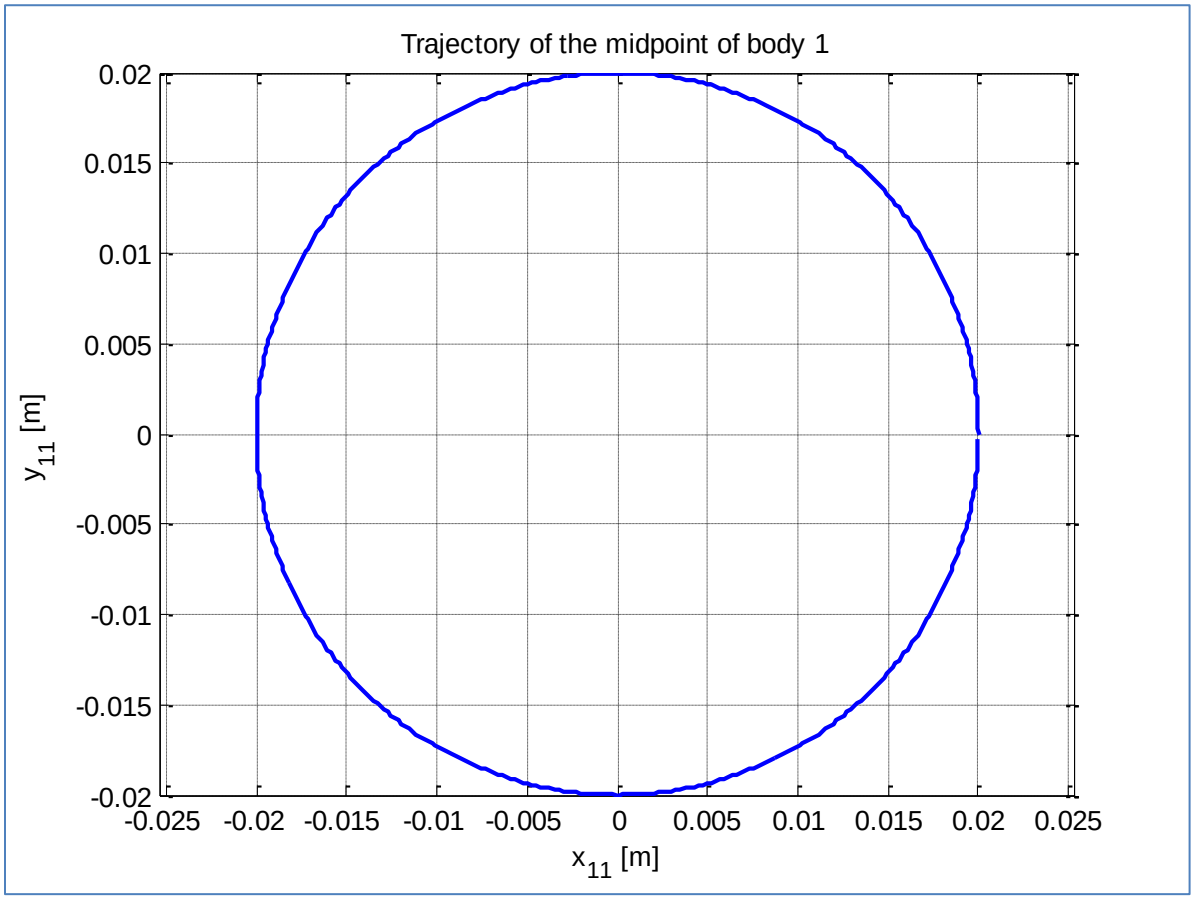

Figure 7 Trajectory of the Midpoint of the Crank.

4.4 KINEMATIC ANALYSIS IN SOLIDWORKS

A slider-crank model was built in Solid Works ™ to compute the kinematic analysis. The main objective of the model was to validate the obtained results from the Matlab code. The tool of Motion Study in SolidWorks was used to compute the kinematic analysis. The position, the velocity and the acceleration analyses were also carried out. The following figure shows the SolidWorks model L_1 and L_2 are defined as 0.04m and 0.08m; L_1 and L_2 are the crank's and the coupler's respective lengths.

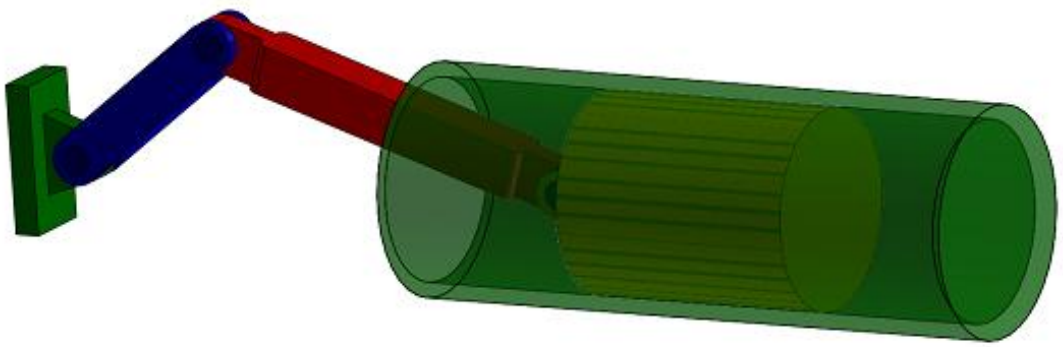

Figure 8 Solid Works Model

The spring constant is defined by k = 1500N/m. Frame, crank, coupler and slider are interconnected by revolute joints. The initial position of the model is when the spring is fully compressed. The Solid Works model also includes the spring. The figure 9 shows the mechanism.

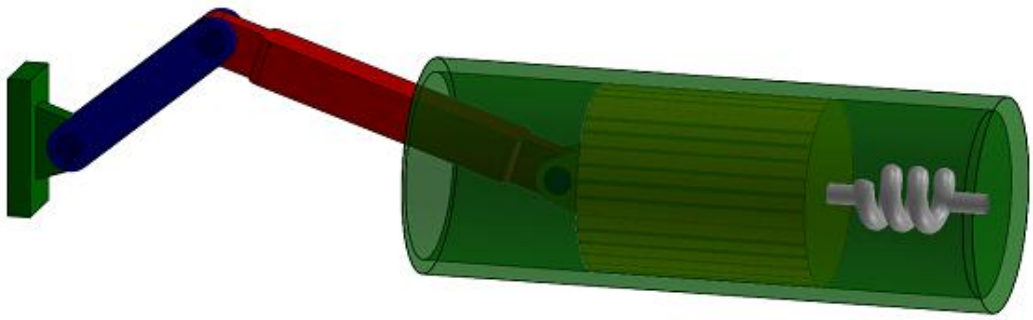

Figure 9 Slider - Crank Model

4.4.1 POSITION ANALYSIS IN SOLIDWORKS

The figure 10 shows the displacement of the slider.

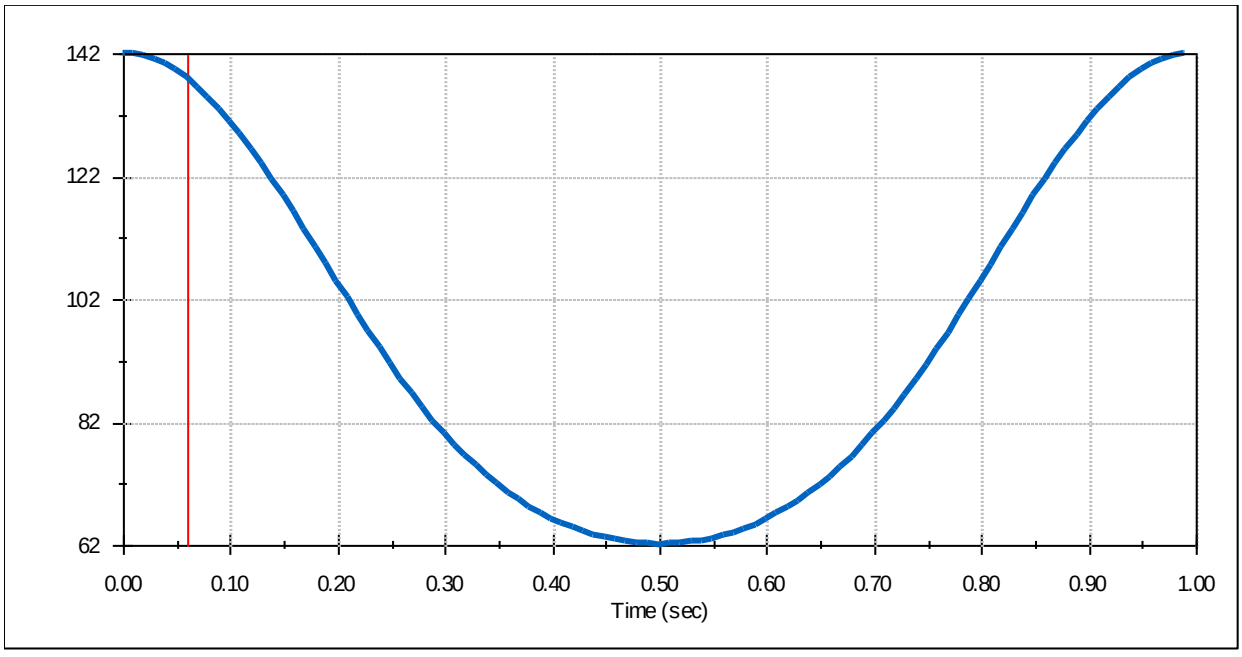

Figure 10 Time vs. Displacement of the Slider in Solid Works

This graph shows the displacement of the slider. The total displacement during one revolution is 80mm.

4.4.2 VELOCITY ANALYSIS IN SOLIDWORKS

The figure 11 shows the velocity of the slider.

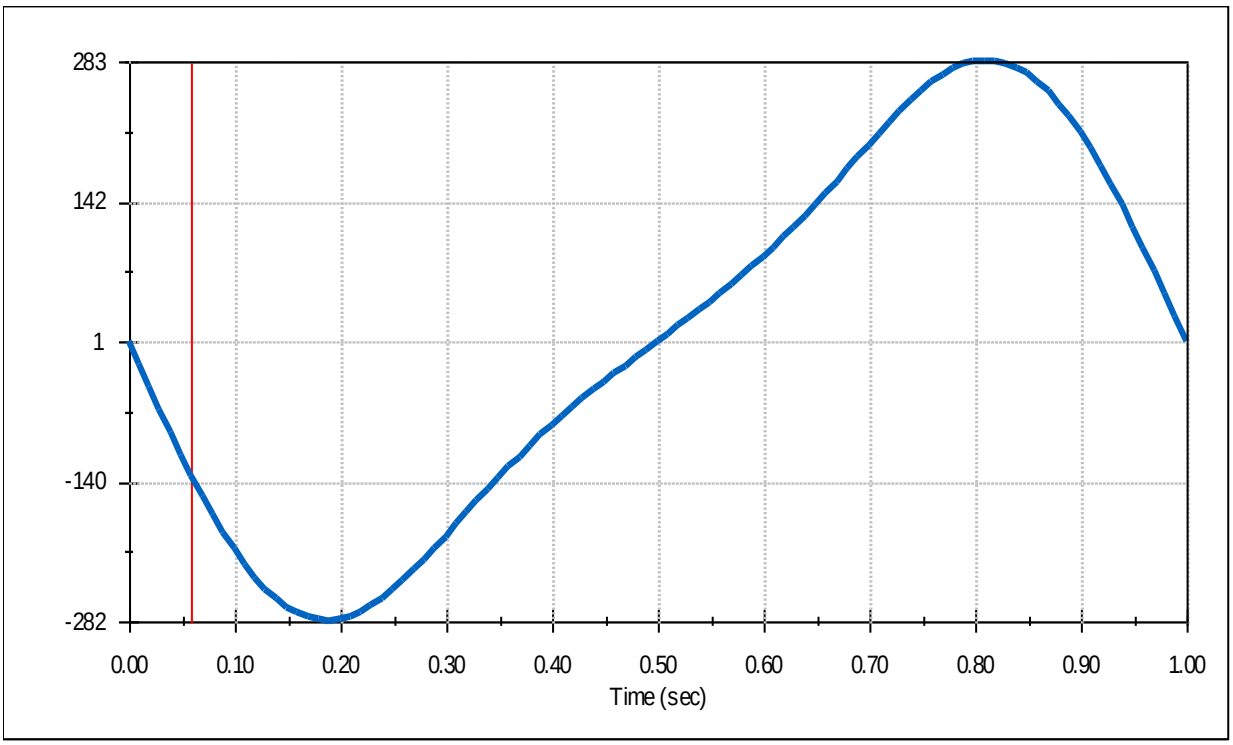

Figure 11 Time vs. Velocity of the Slider in Solid Works

The maximum velocity of the slider is 0.28 m/s and the minimum is - 0.28 m/s. The results from SolidWorks ™ and Matlab™ are exactly the same.

4.4.3 ACELERATION ANALYSIS IN SOLIDWORKS

The figure 12 shows the acceleration of the slider.

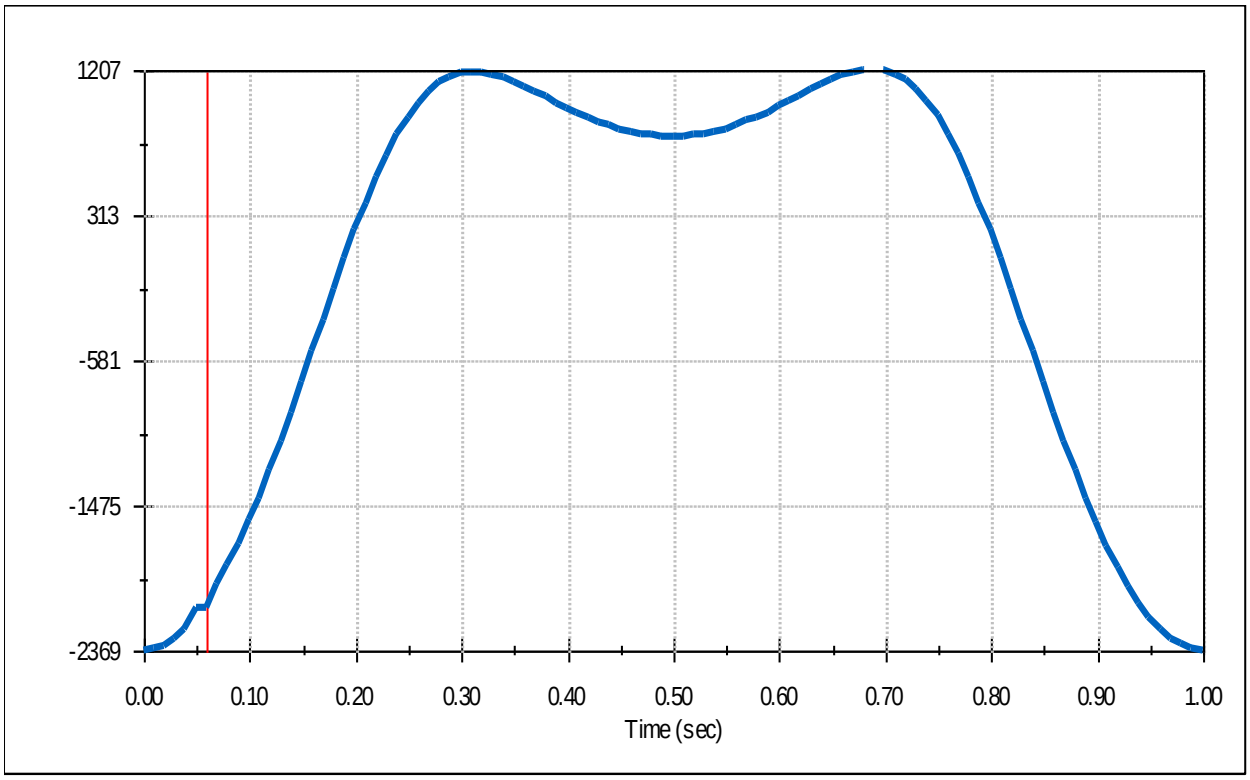

Figure 12 Time vs. Acceleration of the slider in Solid Works

By comparing the kinematic analyses results of the slider – crank model with two programs such as Matlab and Solid Works it is possible to validate the results. The difference between the two approaches is very insignificant which means that the results of the kinematic analyses are reliable.

Chapter 5

DYNAMIC ANALYSIS

The dynamic analysis of the slider – crank mechanism will be developed following the Lagrange multipliers approach. This technique combines the kinematic constraint equations obtained in Chapter 3 and the vector of Lagrange multipliers to create systems of differential equations. It is possible to switch from a constrained optimization problem to an unconstrained one by applying this technique. The unknowns in the system are the vector of Lagrange multipliers (λ) and the vector of generalized accelerations($\ddot{q}$). The generalized reactions in the system can be found with the Lagrange multipliers. The position and the velocities can be determined by integrating the accelerations. [31]

5.1 LAGRANGE METHOD AND THE NEW OBJECTIVE FUNCTION

Pennestri in [30] presented an explanation about the procedure in order to apply the Lagrange multipliers method. First, it is necessary to create a new function which is called objective function which is defined as [30]:

$$L^* = L - \lambda\Psi \qquad \text{Eq. 36}$$

Where L is the Lagrangian function defined as

$$L = T - V \qquad \text{Eq. 37}$$

T represents the kinetic energy and V the potential energy.

The stationary conditions need to be applied to the objective function

$$\frac{\partial L^*}{\partial q_1} \equiv \frac{\partial L}{\partial q_1} - \lambda \frac{\partial \Psi}{\partial q_1} = 0$$

$$\frac{\partial L^*}{\partial q_2} \equiv \frac{\partial L}{\partial q_2} - \lambda \frac{\partial \Psi}{\partial q_2} = 0$$

$$\vdots \qquad \text{Eq. 37}$$

$$\frac{\partial L^*}{\partial q_n} \equiv \frac{\partial L}{\partial q_n} - \lambda \frac{\partial \Psi}{\partial q_n} = 0$$

and

$$\frac{\partial L^*}{\partial \lambda} \equiv \Psi = 0 \qquad \text{Eq. 38}$$

5.2 HAMILTON'S INTEGRAL

The Hamilton's equation which imposed the stationarity of the integral is given by [30]

$$\delta \int_{t_1}^{t_2} L dt = 0 \qquad \text{Eq. 39}$$

Finally, by combining the Hamilton and the Lagrangian principles it is possible to end up with [30]

$$[M]\{\ddot{q}\} + \left[\Psi_q\right]^T \{\lambda\} = \{F_e\} \qquad \text{Eq.40}$$

The proof of the above system is shown in the book Cinematica dei Sistemi Multibody by Pennestri et al. [30] pp. 636 – 637.

Where

$\{\ddot{q}\}$ is the vector of accelerations.

$\{\lambda\}$ is the Lagrange multipliers vector.

$[M]$ is the mass matrix.

$[\Psi_q]$ is the Jacobian matrix.

$\{F_e\}$ is the generalized forces vector.

The mass matrix of a rigid body is defined with respect of the position of the reference point in the body. If the reference point is considered exactly in the same location as the center of mass of the body, the mass matrix is diagonal.

$$M = \begin{bmatrix} M^1 & & & & \\ & M^2 & & 0 & \\ & & \ddots & & \\ & & & M^i & \\ & 0 & & & \ddots \\ & & & & & M^{nb} \end{bmatrix} \quad \text{Eq. 41}$$

The mass matrix of each body is defined by

$$[M^i] = \begin{bmatrix} m^i \mathrm{I} & 0 \\ 0 & {I_G}^i \end{bmatrix} \quad \text{Eq. 42}$$

Where m^i is the mass of the body i and ${I_G}^i$ is the mass moment of inertia defined with respect to the center of mass of the body i.

5.3 DIFFERENTIAL ALGEBRAIC EQUATION SYSTEM

The DAE (Differential – Algebraic Equations) system for the solution of the dynamic analysis is given by [30]

$$\begin{bmatrix} \mathrm{M} & \Psi_q^T \\ \Psi_q & 0 \end{bmatrix} \begin{Bmatrix} \ddot{q} \\ \lambda \end{Bmatrix} = \begin{Bmatrix} F_e \\ \gamma \end{Bmatrix} \quad \text{Eq. 43}$$

In this system the unknowns are the vector of Lagrange multipliers (λ) and the vector of generalized accelerations($\ddot{q}$). The Lagrange multipliers are used to calculate the generalized reaction in the system. The position and the velocity can be determined by integrating the accelerations. In order to solve the system it is necessary to perform the following procedure.

$$\begin{Bmatrix} \ddot{q} \\ \lambda \end{Bmatrix} = \begin{bmatrix} \mathrm{M} & \Psi_q^T \\ \Psi_q & 0 \end{bmatrix}^{-1} \begin{Bmatrix} F_e \\ \gamma \end{Bmatrix} \quad \text{Eq. 44}$$

Then

$$\begin{bmatrix} \mathrm{M} & \Psi_q^T \\ \Psi_q & 0 \end{bmatrix}^{-1} = \begin{bmatrix} A_{qq} & A_{q\lambda} \\ A_{\lambda q} & A_{\lambda\lambda} \end{bmatrix} \quad \text{Eq. 45}$$

Where

$$[A_{\lambda\lambda}] = ([\Psi_q][M]^{-1}[\Psi_q]^T)^{-1} \quad \text{Eq. 46}$$

$$[A_{qq}] = [M]^{-1} - M^{-1}[\Psi_q]^T[A_{\lambda\lambda}]\Psi_q M^{-1} \quad \text{Eq. 47}$$

$$[A_{q\lambda}] = -[M]^{-1}[\Psi_q]^T[A_{\lambda\lambda}] = [A_{\lambda q}]^T \quad \text{Eq. 48}$$

Finally, the accelerations and the Lagrange multipliers are given by

$$\{\ddot{q}\} = [A_{qq}]\{F_e\} + [A_{q\lambda}]\{\gamma\} \quad \text{Eq. 49}$$

$$\{\lambda\} = [A_{\lambda q}]\{F_e\} + [A_{\lambda\lambda}]\{\gamma\} \quad \text{Eq. 50}$$

5.4 DYNAMIC ANALYSIS

To compute the dynamic analysis of a slider crank mechanism shown in Figure 1 is necessary to determine the mass matrix of the system [M], the Jacobian $[\Psi_q]$ of the constraint equation vector, the external forces vector $\{F_e\}$ and the gamma vector $\{\gamma\}$. These dynamic equations are expressed bellow.

5.4.1 MASS MATRIX

The system is composed by three bodies, and since the local reference frame for each body is located in the center of mass, the mass matrix is diagonal. The final mass matrix is shown below. Where m_{cr} and I_{cr} are equal to the mass and the inertia of the crank, m_{co} and I_{co} are equal to the mass and inertia of the connecting road, and, finally m_{sl} and I_{sl} are the masses and inertias of the slider.

$$[M] = \begin{bmatrix} m_{cr} & 0 & 0 & 0 & 0 & 0 & 0 & 0 & 0 \\ 0 & m_{cr} & 0 & 0 & 0 & 0 & 0 & 0 & 0 \\ 0 & 0 & I_{cr} & 0 & 0 & 0 & 0 & 0 & 0 \\ 0 & 0 & 0 & m_{co} & 0 & 0 & 0 & 0 & 0 \\ 0 & 0 & 0 & 0 & m_{co} & 0 & 0 & 0 & 0 \\ 0 & 0 & 0 & 0 & 0 & I_{co} & 0 & 0 & 0 \\ 0 & 0 & 0 & 0 & 0 & 0 & m_{sl} & 0 & 0 \\ 0 & 0 & 0 & 0 & 0 & 0 & 0 & m_{sl} & 0 \\ 0 & 0 & 0 & 0 & 0 & 0 & 0 & 0 & I_{gs} \end{bmatrix}$$

Eq. 51

Where the values for the mass and the inertia of each body are shown in the following table

	Crank	**Coupler**	**Slider**
Mass [kg]	0.01432	0.07767	0.0264
Inertia [kg*m^2]	2.7 x 10^{-6}	4.59x10^{-5}	2.112x10^{-5}

Table 1 Masses and Inertias

5.4.2 JACOBIAN OF THE CONSTRAINT EQUATION VECTOR

The Jacobian matrix $[\Psi_q]$ has been determined in the velocity and the acceleration analysis in chapter 4.2.6

$$[\Psi_q] = \begin{bmatrix} 1 & 0 & \frac{L_1}{2}\sin q_3 & 0 & 0 & 0 & 0 & 0 & 0 \\ 0 & 1 & -\frac{L_1}{2}\cos q_3 & 0 & 0 & 0 & 0 & 0 & 0 \\ 1 & 0 & -\frac{L_1}{2}\sin q_3 & -1 & 0 & -\frac{L_2}{2}\sin q_6 & 0 & 0 & 0 \\ 0 & 1 & \frac{L_1}{2}\cos q_3 & 0 & -1 & \frac{L_2}{2}\cos q_6 & 0 & 0 & 0 \\ 0 & 0 & 0 & 1 & 0 & -\frac{L_2}{2}\cos q_6 & -1 & 0 & 0 \\ 0 & 0 & 0 & 0 & 1 & \frac{L_2}{2}\cos q_6 & 0 & -1 & 0 \\ 0 & 0 & 0 & 0 & 0 & 0 & 0 & 1 & 0 \\ 0 & 0 & 0 & 0 & 0 & 0 & 0 & 0 & 1 \end{bmatrix} \quad \text{Eq. 52}$$

Where L_1 and L_2 are the crank and the coupler lengths respectively. L_1 = 0.040 m and L_2 = 0.080m.

5.4.3 EXTERNAL FORCES VECTOR

In the following analysis the force which is acting on the system is the one which is produced by the spring element. The spring is interconnected to the slider; its initial position is when the spring is compressed. The information of the spring is shown in the table 2.

Stiffness K (N/m^2)	**D_{max} (m)**	**N**
1500	0.150	3

Table 2 Spring Properties

5.4.4 GAMMA VECTOR

The gamma vector for the mechanism was developed in the kinematic analysis and is defined as

$$\{\gamma\} = \begin{Bmatrix} -\frac{L_1}{2}\dot{q_3}^2 \cos q_3 \\ -\frac{L_1}{2}\dot{q_3}^2 \sin q_3 \\ \frac{L_1}{2}\dot{q_3}^2 \cos q_3 + \frac{L_2}{2}\dot{q_6}^2 \cos q_6 \\ \frac{L_1}{2}\dot{q_3}^2 \sin q_3 + \frac{L_2}{2}\dot{q_6}^2 \sin q_6 \\ \frac{L_2}{2}\dot{q_6}^2 \cos q_6 \\ \frac{L_2}{2}\dot{q_6}^2 \sin q_6 \\ 0 \\ 0 \end{Bmatrix} \quad \text{Eq. 53}$$

5.4.5 INITIAL CONDITIONS FOR THE DYNAMIC ANALYSIS

The initial position of the mechanism is defined with an initial crank's angle of θ1 = 34.19°. A study was developed in collaboration with Lorenzo Mariti et al. [32] which established that the maximum value of angular velocity is found with the following initial configuration.

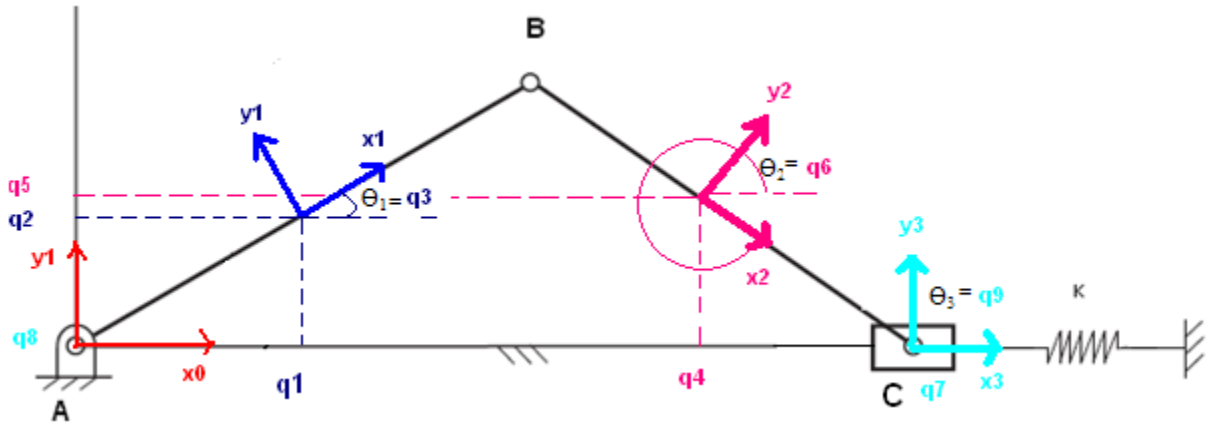

Figure 13 Initial Configuration

With the optimum initial conditions the generalized coordinates are defined as

$$q_1 = \frac{L_1}{2}\cos\Theta\,\theta_1 \quad \text{Eq. 54}$$

$$q_2 = \frac{L_1}{2}\sin\Theta\,\theta_1 \quad \text{Eq. 55}$$

$$q_3 = \theta_1 \quad \text{Eq. 56}$$

$$q_4 = L_1\cos\Theta\,\theta_1 + \frac{L_2}{2}\cos\Theta\,\theta_2 \quad \text{Eq. 57}$$

$$q_5 = -\frac{L_2}{2}\sin\Theta\,\theta_2 \quad \text{Eq. 58}$$

$$q_6 = \theta_2 \quad \text{Eq. 59}$$

$$q_7 = \frac{L_1}{2}\cos\Theta\,\theta_1 + \frac{L_2}{2}\cos\Theta\,\theta_2 \quad \text{Eq. 60}$$

$$q_8 = 0 \quad \text{Eq. 61}$$

$$q_9 = 0 \quad \text{Eq. 62}$$

Where $\Theta\,\theta_2$ is defined as

$$\Theta\,\theta_2 = \sin^{-1}\left(\frac{L_1\sin\Theta\,\theta_1}{L_2}\right) \quad \text{Eq. 63}$$

5.5 SOLVING THE SYSTEM

In order to solve the DAE (Differential Algebraic Equation) system in Eq. 43, a Matlab code was developed to find the unknowns: the vector of Lagrange multipliers (λ) and the vector of generalized accelerations($\ddot{q}$).The solutions for position, velocities and accelerations were found. In addition the reaction forces in the joints were calculated as well.

5.5.1 POSITION, VELOCITY AND ACCELERATION OF THE CRANK

The position of the crank is described by the figure 14.

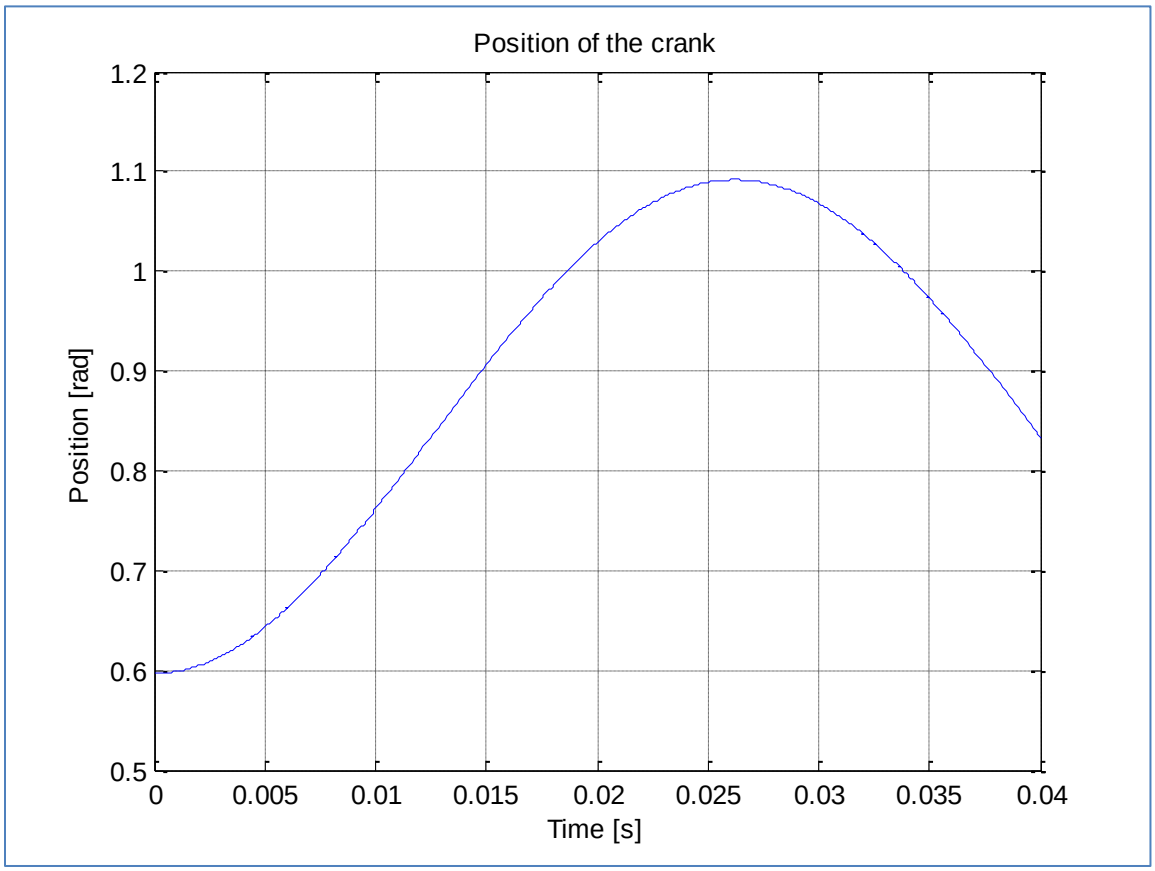

Figure 14 Time vs. Position of the Crank Link

The maximum value is reached at 0.0265 s (approx.) when the angle of the crank is 1.09 rad (approx.). Furthermore, the displacement of the slider in .0265s is defined as 0.022 m.

The velocity of the crank is given by figure 15

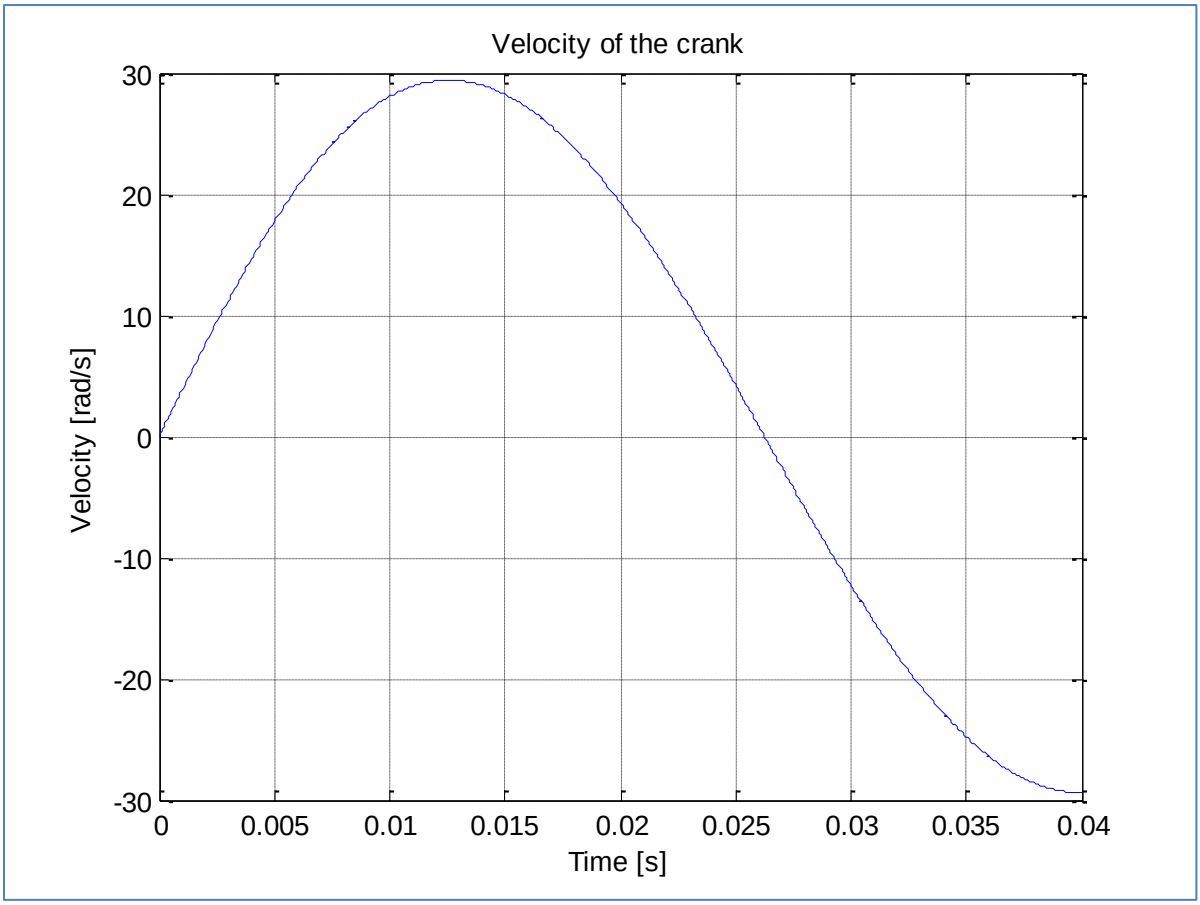

Figure 15 Time vs. Velocity of the Crank Link

The maximum value of the velocity (29 rad/s) is reached in 0.013 s.

The acceleration of the crank is shown in the next graph

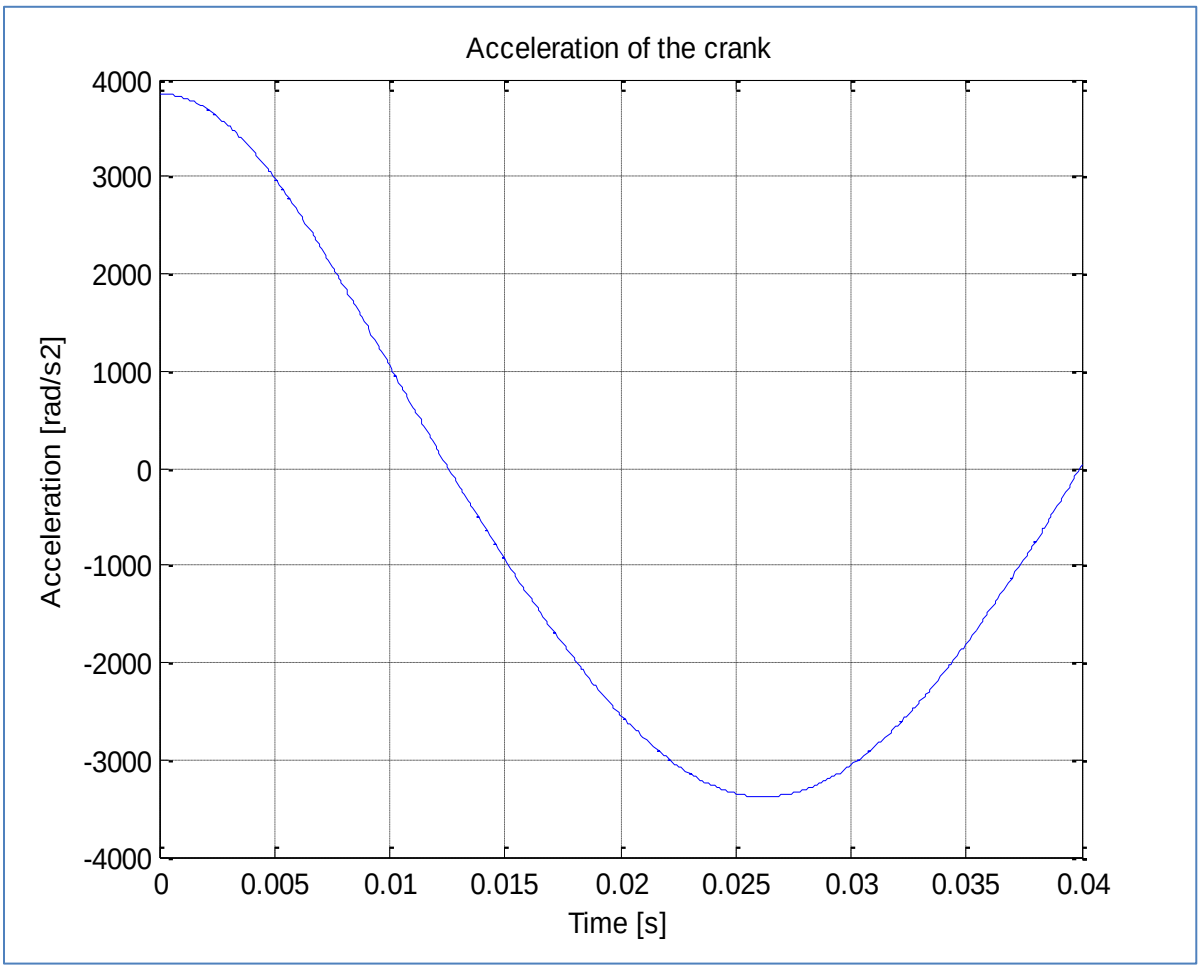

Figure 16 Time vs. Acceleration of the crank

The computation of the norm of the constraint equations was carried out to verify the results. The norm of the constraint equation is a measure of how the constraints are

satisfied; it is strongly related to the length unit which is used in the model (m). In other words, if the norm is 2 x 10^{-8} m and your length unit in meter, it means that you have an average error on the constraint that is equal to 2 x 10^{-8} m. This parameter can be adjusted by acting on the integration tolerance or using a stabilization technique. The sense of the stabilization technique is, in fact, to damp the oscillation of the norm of the constraint equations. As shown in the figure, the values of the norm of the constraint equations are very close to zero. It means the results are reliable and acceptable.

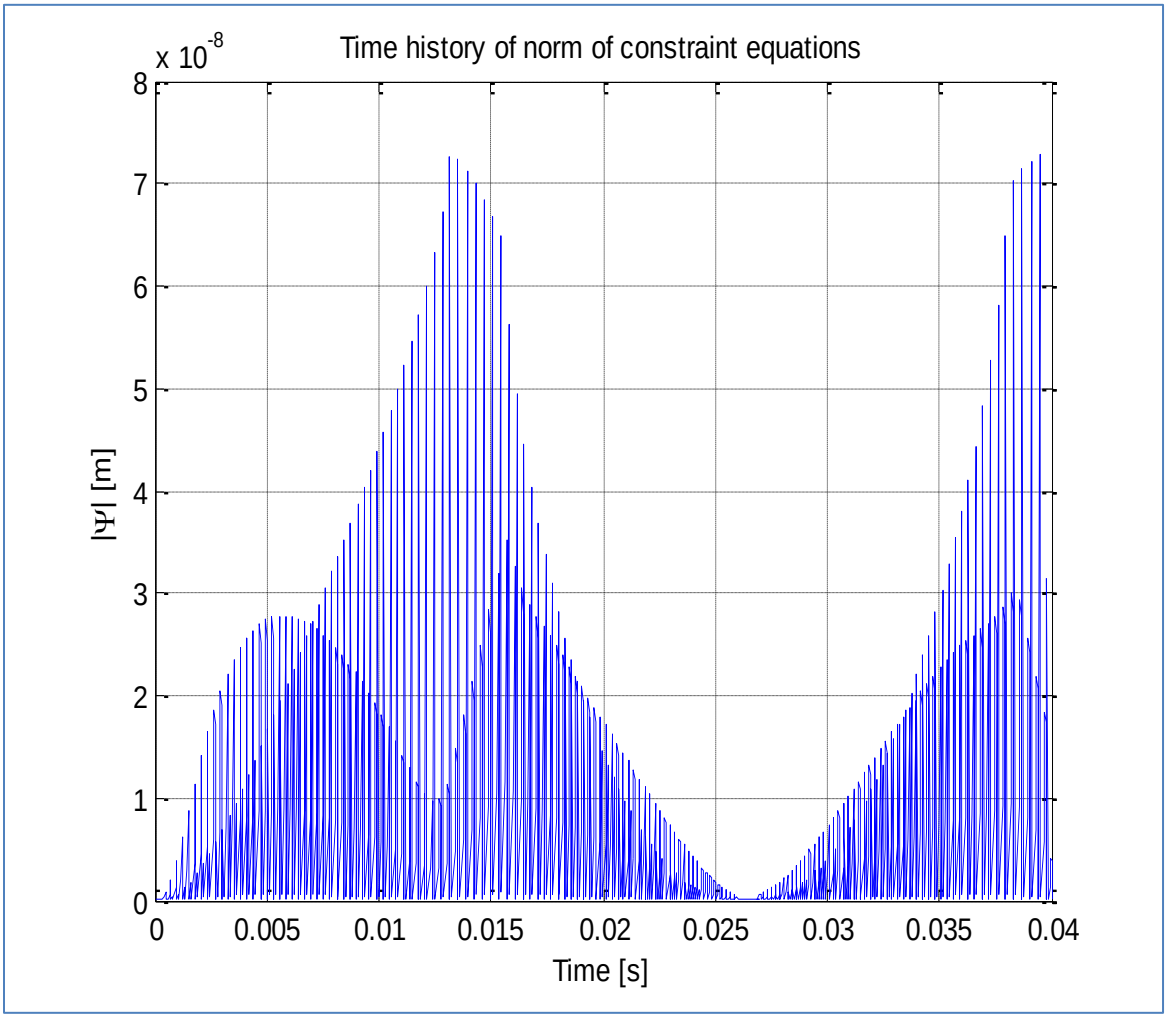

Figure 17 Time vs. Norm of Constraint Equation

Furthermore, the trajectory of the midpoint of the crank is also very useful to check the reliability of the results. If the results are correct the midpoint of the crank needs to trace a circle.

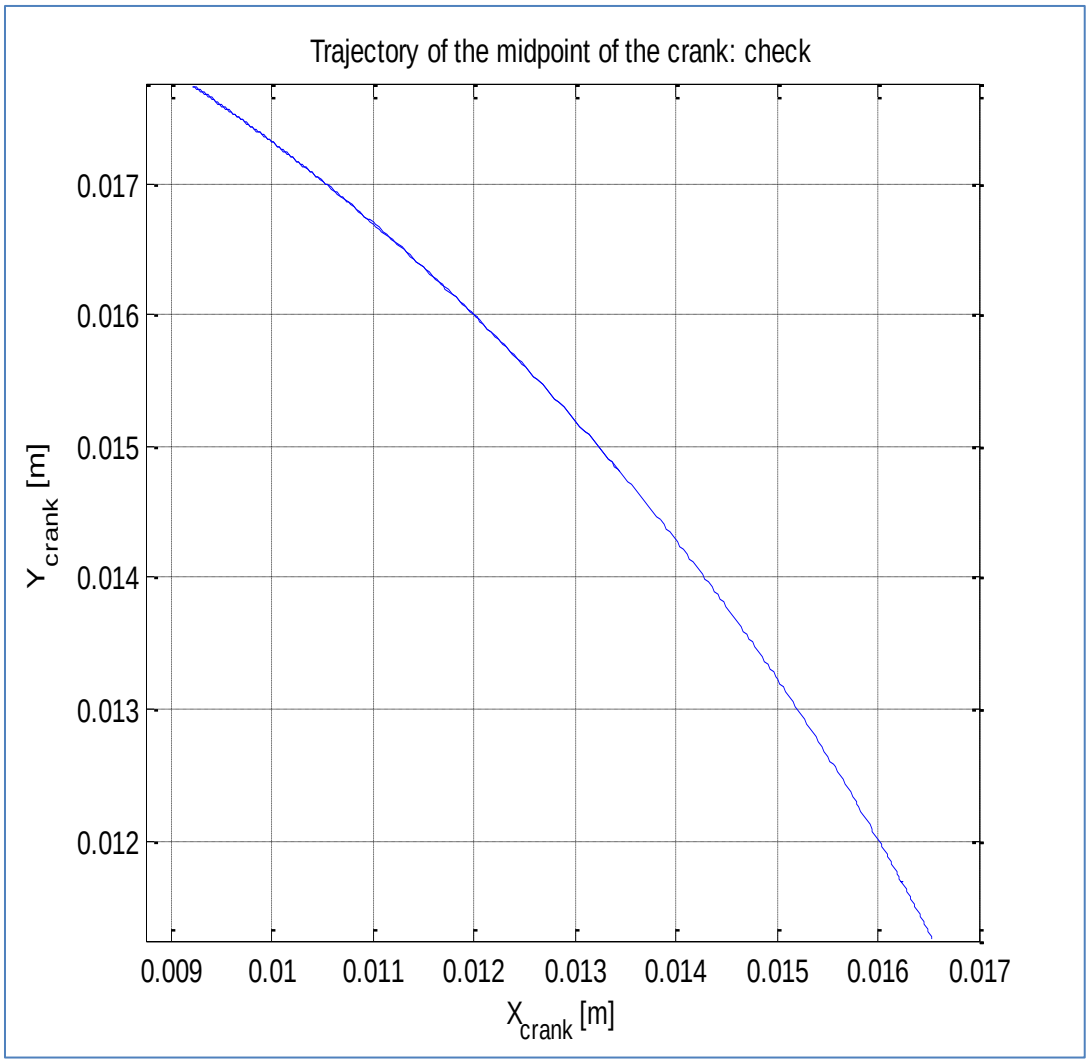

Figure 18 Trajectory of the Midpoint of the Crank

5.5.2 POSITION OF THE SLIDER

The displacement of the slider crank is described in the following graph. The maximum displacement of the slider (0.11m) is given when the mechanism is in its initial position.

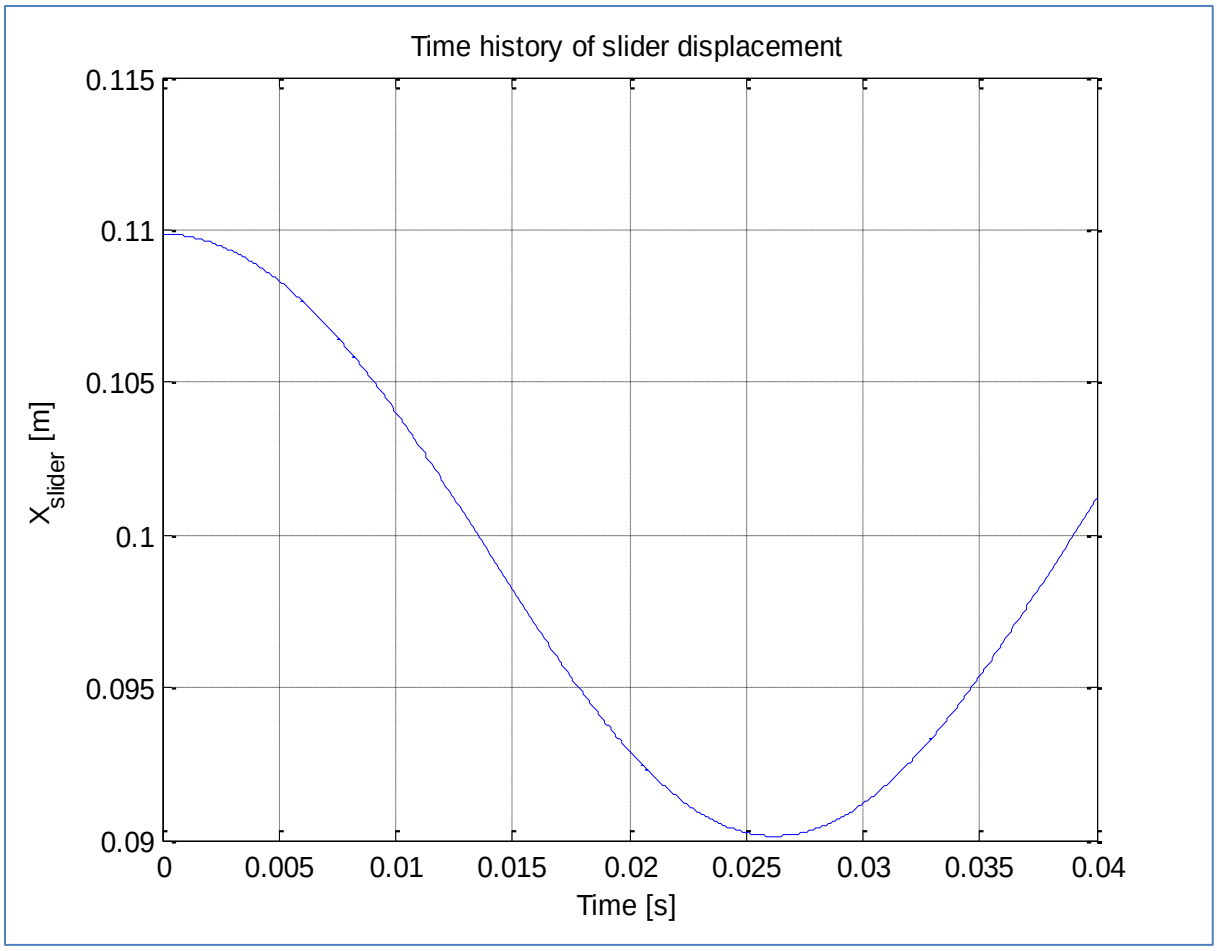

Figure 19 Time vs. Displacement of the Slider

5.5.3 REACTION FORCES AT THE JOINTS

The reaction forces acting on the crank's joint A (see figure 1) acting is given by

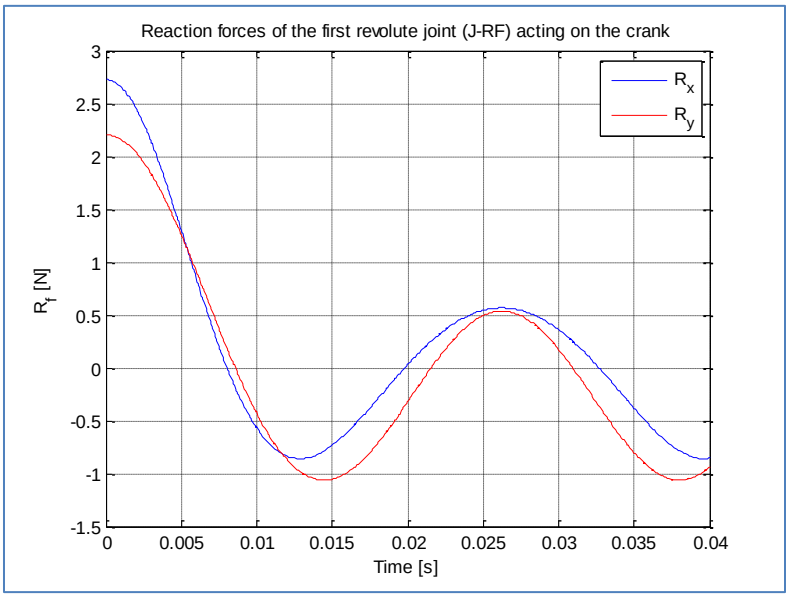

Figure 20 Reaction Force at Joint A on the Crank

The reaction forces in the revolute joint B acting on the crank is described by:

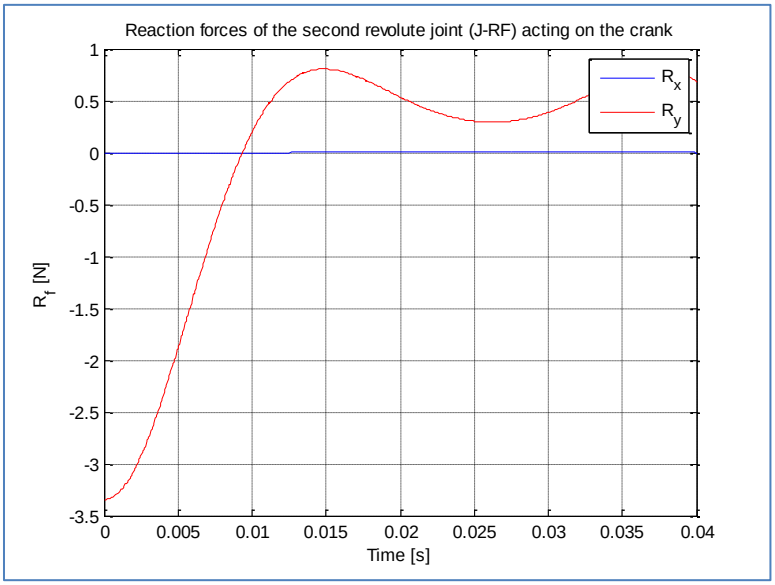

Figure 21 Reaction Force at joint B on the Crank

The reaction forces in the revolute joint B (see figure 1) acting on the coupler is shown in the next graph.

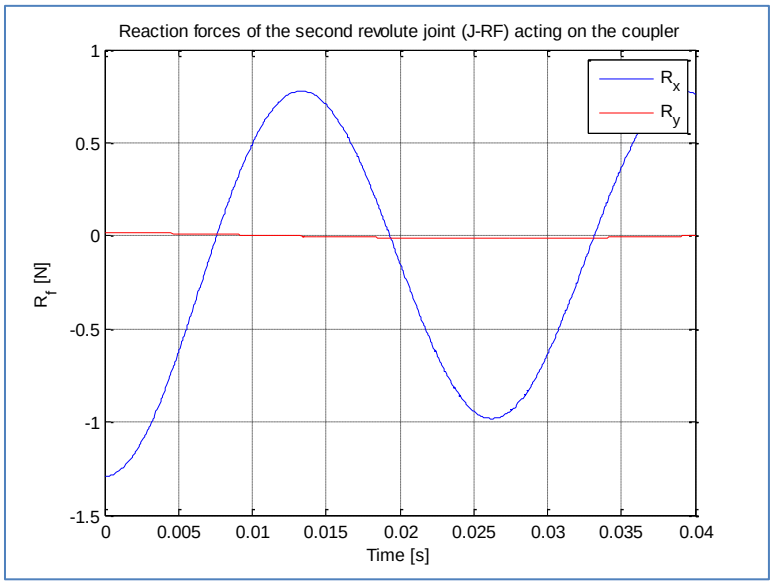

Figure 22 Reaction Force at Joint B Acting on the Coupler

Finally, the comparison of the modulus of the second revolute joint reaction forces is given by

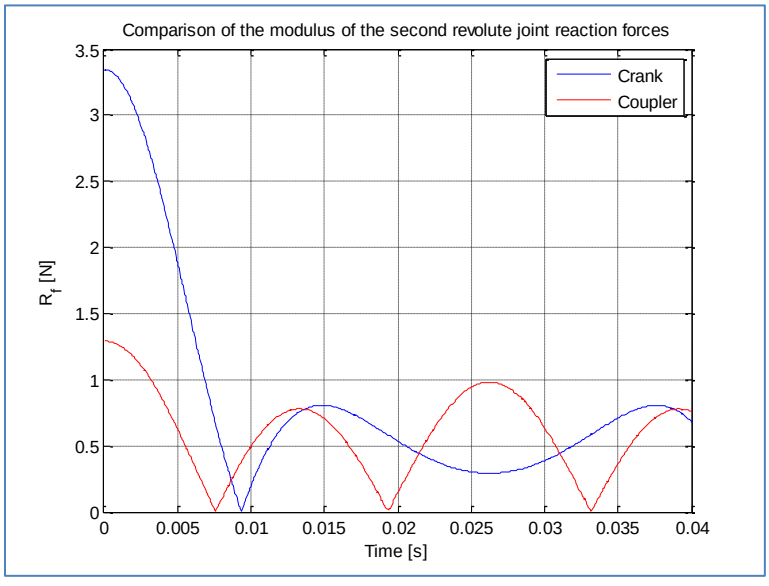

Figure 23 Modulus at Joint B (reaction forces)

Chapter 6

Considerations of Design and Application

Chapter 6 studies some components of the mechanism in order to analyze their behavior under certain loads and conditions; the finite element method is applied on different parts to study stresses, deformations, vibrations and more. Those analyses are necessary to determine any possible failure in the system. By the implementation of a commercial software ABAQUS ^{TM} , it is possible to analyze such values. Furthermore, this software allows running explicit dynamic simulations which are needed in this research.

6.1 FINITE ELEMENT ANALYSIS OF A SPRING IN ABAQUS

An Explicit Dynamic Analysis is performed to analyze the spring in the slider crank mechanism; First, the spring is subjected to an initial displacement of .0221m.Second, the mechanism is released and the spring changes from the compressed position to the final configuration (uncompressed position). Finally, the spring bounces for a certain period of time. A commercial software (ABAQUS ^{TM}) is implemented to carry out the Finite Element Analysis to determine any possible failure in the spring.

The analyzed spring has the following characteristics which were obtained from a helical spring optimization process. This procedure is presented in the study developed by Mariti et al. in [32]; this study was based on a dynamic optimization process to design the spring taking into consideration the dynamic and structural aspects. The characteristics of the spring are given by:

- Stiffness 1500 N/m
- Free length 0.043 m
- Wire diameter .0044 m
- Spring diameter: 0.150m
- Minimum Number of coils: 3

The objective of the Explicit Dynamic Analysis in ABAQUS is to validate the calculation of the spring carried out in the helical spring optimization process in [32]. The data presented above is the minimum number of coils that the spring needs to move 22mm the slider in the mechanism. The figure 24 shows the drawings of the spring.

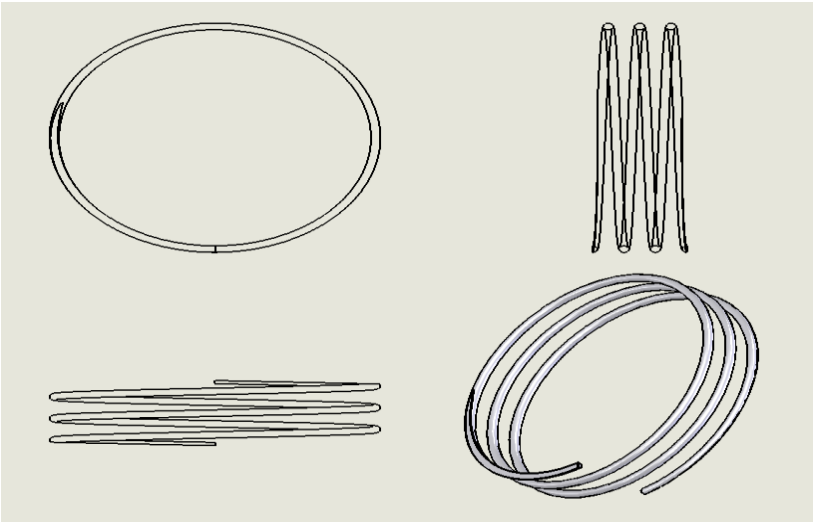

Figure 24 Drawing of the spring

6.1.1 ABAQUS MODEL

The model developed in ABAQUS™ consists in three bodies: the top plate, spring and bottom plate.

1. **The top plate:** The top plate is defined as a rigid body with the following characteristics. This square plate was created in ABAQUS ™ with a dimension of 0.160m. The mesh of the top plate consists of 100 elements and 123 nodes.

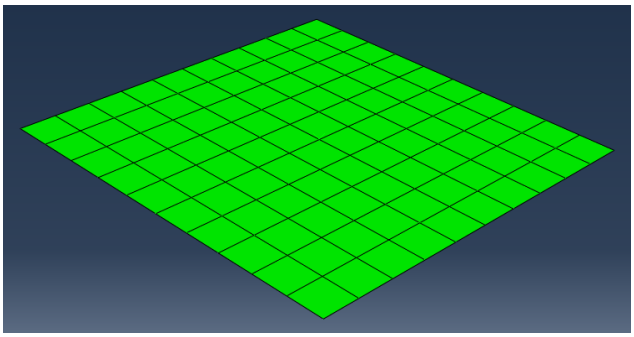

Figure 25 Top Plate

2. **The Spring:** The spring was modeled in the commercial software known as Solid Works ™. Then, the geometry was imported into ABAQUS ™ to continue with the FEA. The mesh of the spring has 822 elements and 517 nodes. The spring has the following material properties:

Material	Music Wire ASTM A 228
Modulus of Elasticity	206 842 710 000Pa
Density	7861.09 kg/m^3

Table 3 Material Properties of the Spring

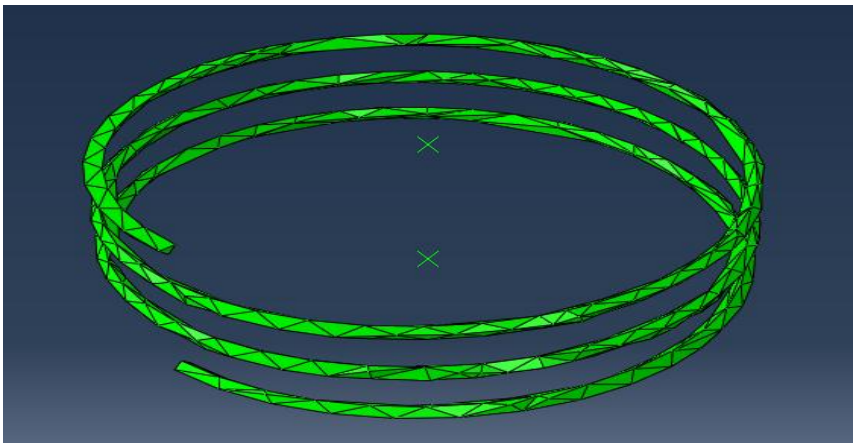

Figure 26 Spring Model in ABAQUS

1. **The Bottom plate:** The bottom plate is defined as a rigid body with the similar characteristics as the top plate. The squared plate was designed in ABAQUS ™ with a dimension of 0.160 m. The bottom plate mesh consists of 100 elements and 123 nodes.

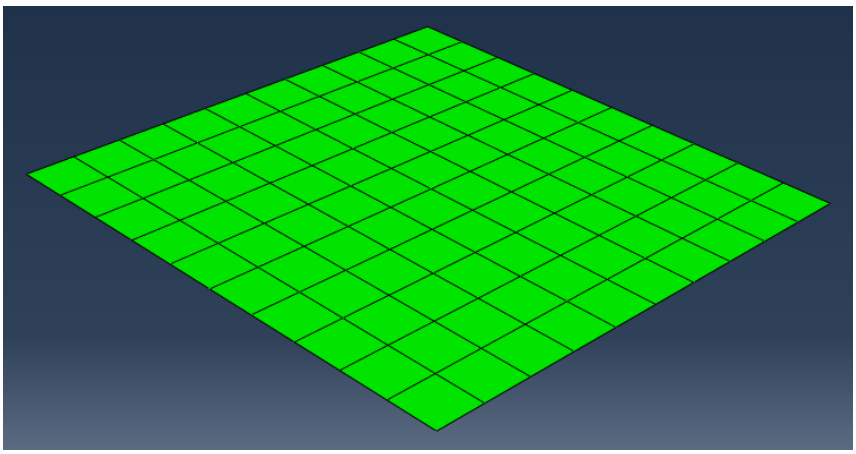

Figure 27 Bottom Plate in ABAQUS

6.1.2 FINAL MODEL

The final model is defined by 1022 elements and 750 nodes.

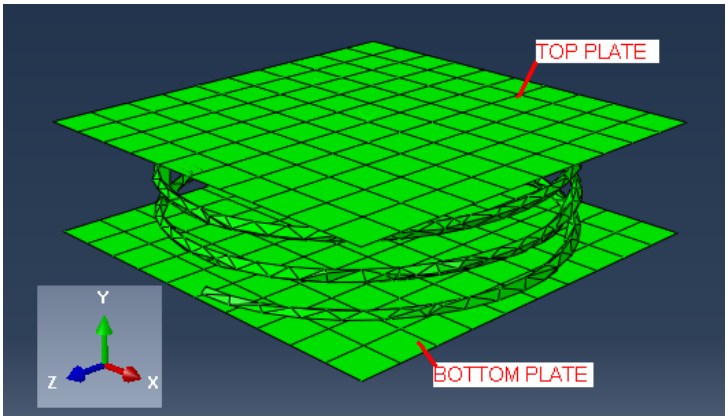

Figure 28 Final Model in ABAQUS

6.1.3 BOUNDARY CONDITIONS

6.1.3.1 LOADS AND DISPLACEMENT.

- A displacement of -0.022m is applied in the Y direction to the top plate.
- The model has not taken in consideration the gravity.
- The bottom plate is fixed in all its degrees of freedom.

6.1.3.2 CONTACT INTERACTIONS

- A mechanical contact was established between the plates and the spring. The contact is friction less and with a tangential behavior.

6.1.4 JOB DESCRIPTION

The final job for the FEA is described by table 4.

STEP1	STEP 2
Contact between bottom plate and spring.	Contact between bottom plate and spring
Contact between top plane and spring.	Deactivate top plate and remove contact between them.
Displacement of -0.022 in Y direction	

Table 4 Description of the Final Job

6.1.5 RESULTS

The displacement of the top plate is defined by the figure 29. The graph shows some peaks and straight lines because the time intervals are not small enough in order to show the real dynamic response of the system. However, the graph shows an approximation of the real curve which describes the behavior of the system.

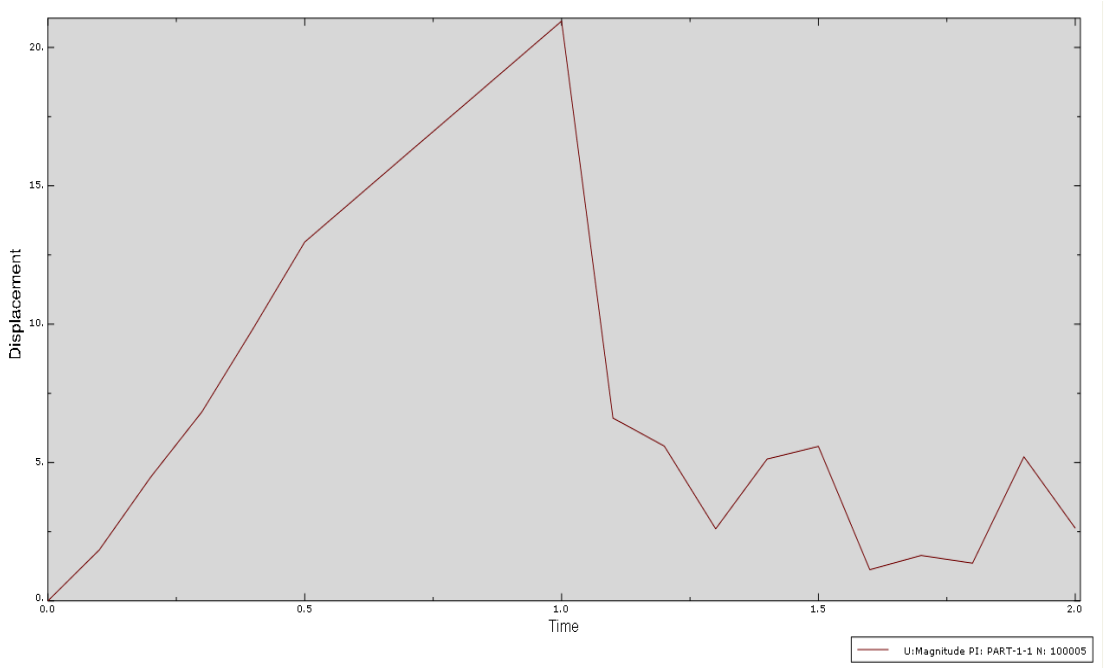

Figure 29 Time vs. Displacement of the top plate.

The Von Mises stress of the spring for different time steps is shown in the figure 30 and 31.

- ✓ **Time step 0.5**

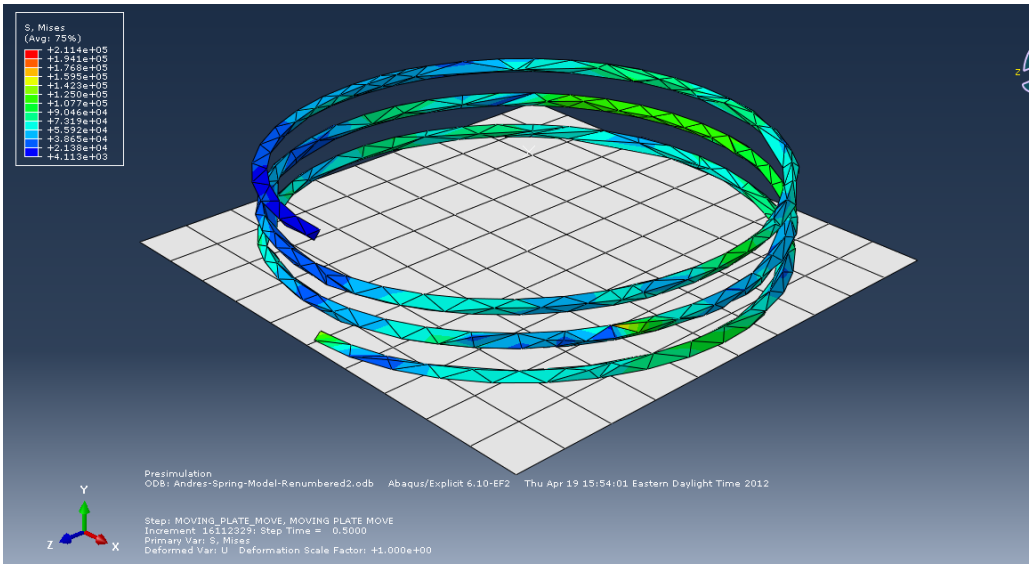

Figure 30 Von Mises stress for step 0.5

- ✓ **Time step 1.** When the displacement (-22 en Y direction) is applied completely

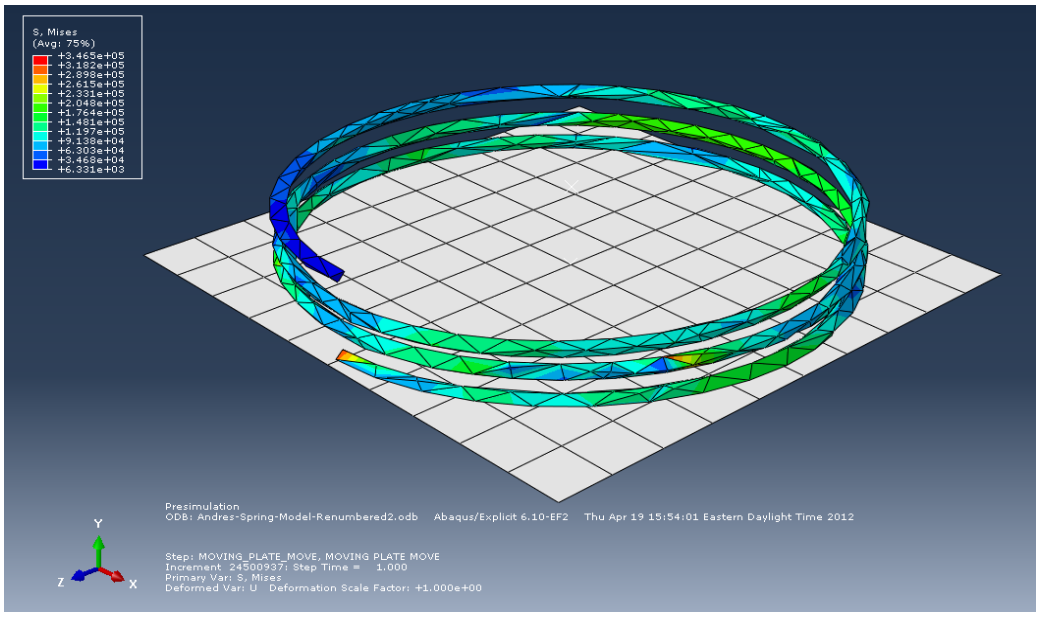

Figure 31 Von Mises Stress for Step 1

✓ **Time step 1.01.**

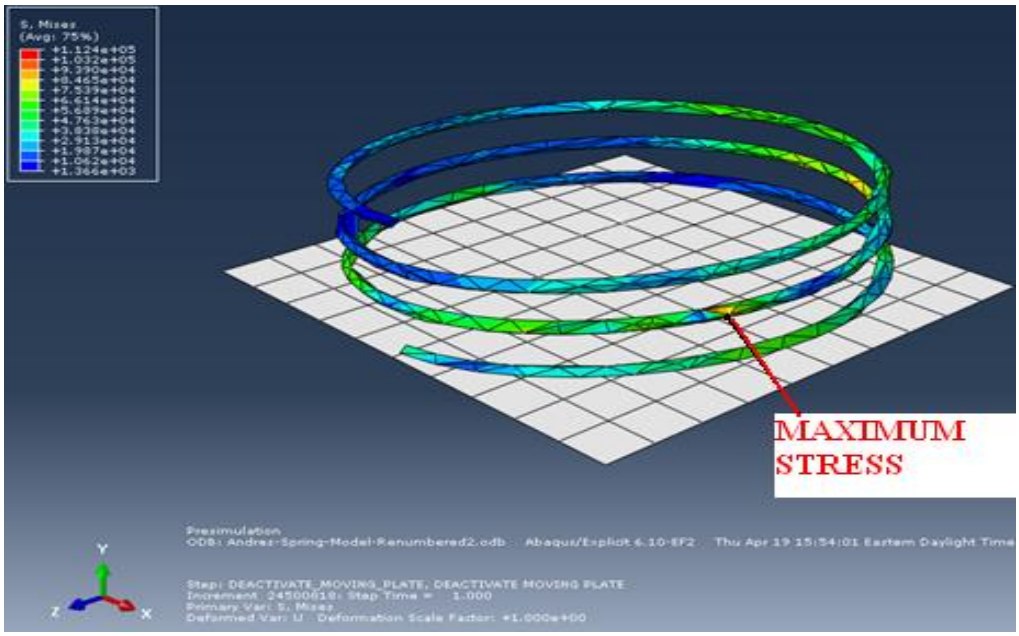

Figure 32 Von Mises Stress for Step 1.01

The figure 32 shows a critical element with a higher stress than the other elements at the time step 1.01. This maximum stress zone was generated because of the vibration in the spring at that specific time step; the direction and velocity that the waves are propagated generate a different response in some elements in the spring. In addition, the quality of the mesh is not the optimum; it is possible to obtain more accurate results if the mesh is redefined with smaller elements in the model. However, it implies more processing time running the analysis.

The Von Mises and maximum principal values of stress for this element are described by:

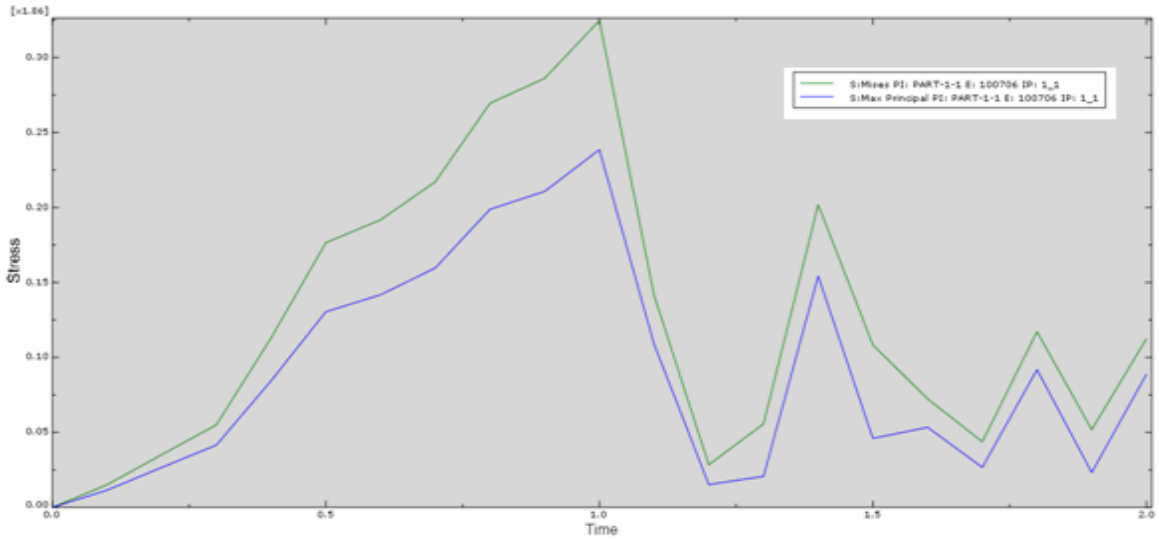

Figure 33 Von Mises and Max. Principal Values of stress for a critical element

The third invariant stress for the maximum stress region is described by:

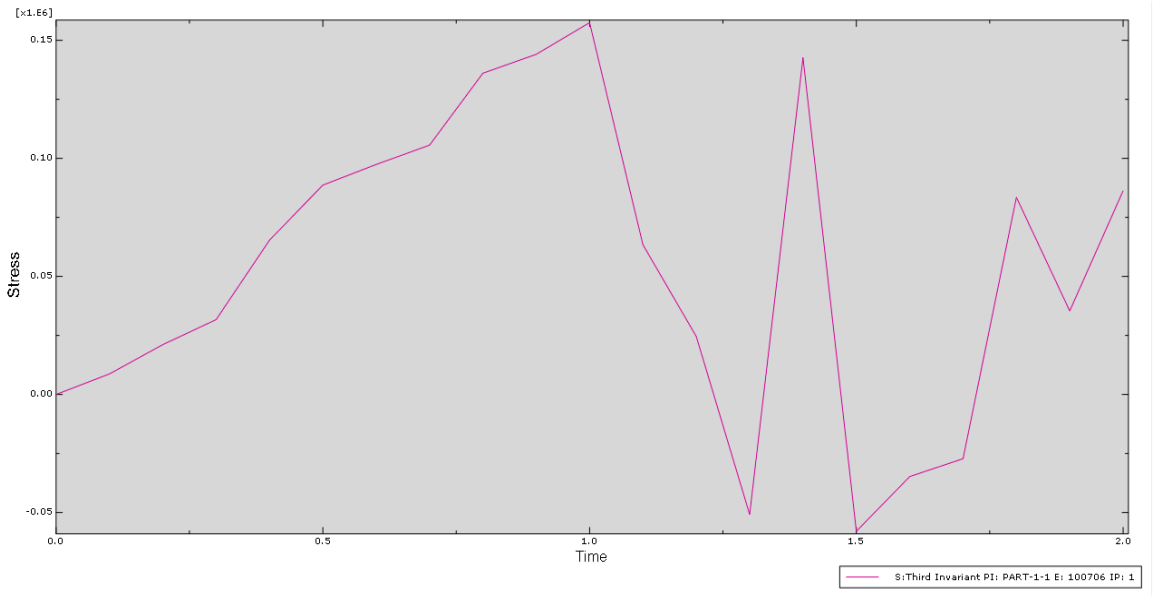

Figure 34 Third Invariant Stress for a Critical Element

The graphs 33 and 34 show some peaks and straight lines because the time intervals are not small enough in order to show the real dynamic response of the system. However, the graphs show an approximation of the real curve which describes stresses of the critical element.

The results of the explicit dynamic analysis developed in ABAQUS for the spring show that the spring will not fail with the loads and displacements applied in the model. In summary, the spring can support the loads applied on it.

6.2 RIGID OR FLEXIBLE BODIES CRITERION IN A HIGH SPEED SLIDER- CRANK DEPLOYMENT MECHANISMS.

A criterion to define the use of rigid or flexible bodies in High Speed Deployment Mechanisms has not been found in the literature review. The next section presents some analyses to establish a parameter to identify the use of rigid or flexible bodies in a Slider-Crank Deployment Mechanism. Transient analyses were developed for four different models to point out the differences among them. Base on the results of those analyses a statement is proposed about how to differentiate between the implementation of rigid or flexible bodies in High Speed Deployment Mechanisms.

First, the slider crank mechanism was analyzed with four different thicknesses on the links in four different models. Second, the forces and moment acting in the coupler link were determined using the motion study tool in SolidWorks^{TM}. Finally, transient

analyses were developed to study each of the models. The table 5 describes the characteristics of the four models of the coupler link with different thicknesses:

	Bodies	Dimensions (m)	Frequency	T (period)	n
MODEL 0	Flexible	0.08 x 0.01 x 0.001	2247.04282	0.00044503	36
MODEL 1	Rigid	0.08 x 0.01 x 0.003	6741.12847	0.00014834	108
MODEL 2	Rigid	0.08 x 0.01 x 0.005	11235.2141	0.000089006	181
MODEL 3	Rigid	0.08 x 0.01 x 0.01	22470.4282	0.000044503	362

Table 5 Models Description

Where n is the number of times that the natural period is smaller than the deployment time (Δt = 0.016128s).

6.2.1 DETERMINATION OF ACCELERATIONS FOR MODEL 0

The acceleration in x and y in the coupler link were determined with the implementation of the motion study tool in Solid Works. The graph 35 shows the acceleration in x

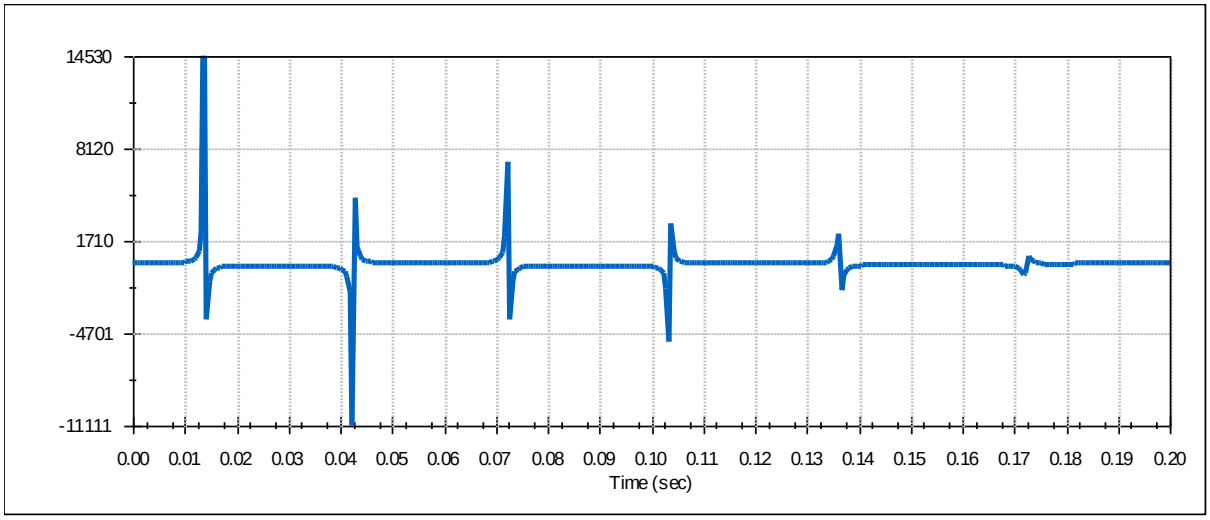

Figure 35 Acceleration in x of the Midpoint of the Coupler Link

The acceleration in y is given by the figure 36.

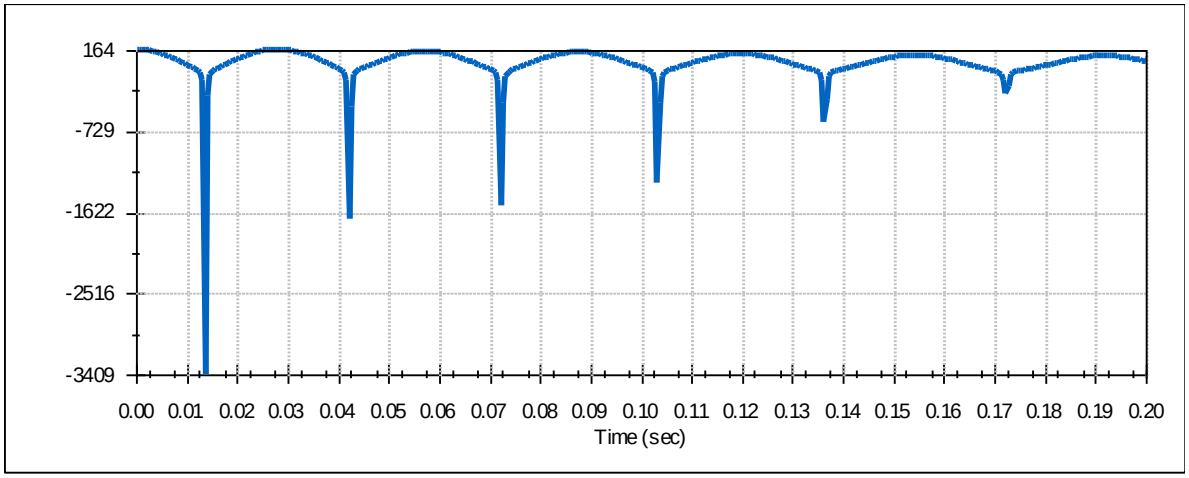

Figure 36 Model1 - Acceleration in y of the Midpoint of the Coupler Link

6.2.2 DETERMINATION OF ACCELERATIONS FOR MODEL1

The acceleration in x and y in the coupler link were determined with the implementation of the motion study tool in Solid Works. The graph 37 shows the acceleration in x

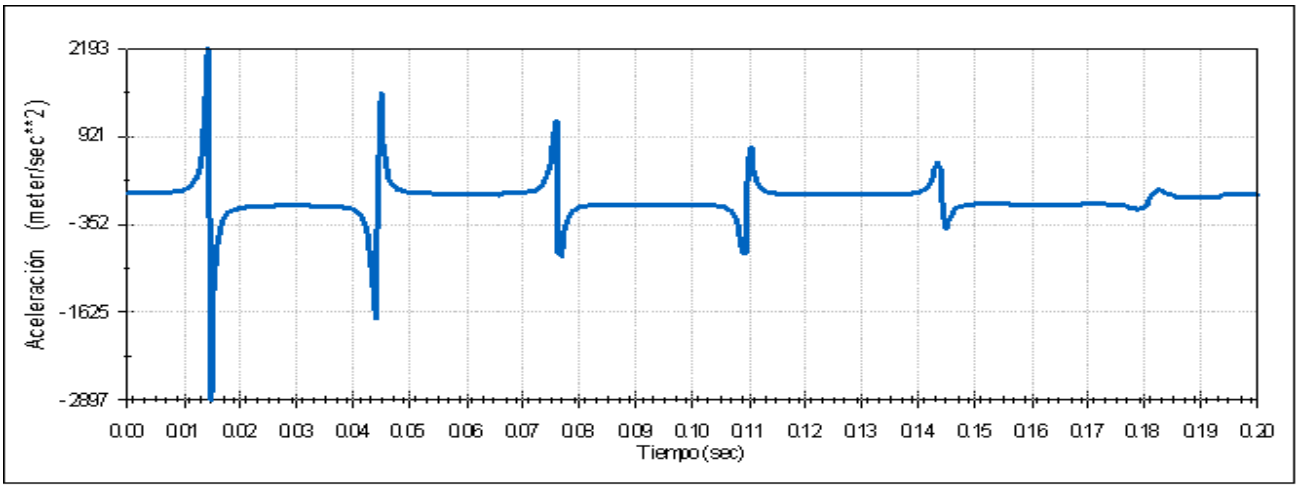

Figure 37 Acceleration in x of the Midpoint of the Coupler Link

The acceleration in y is given by the figure 38.

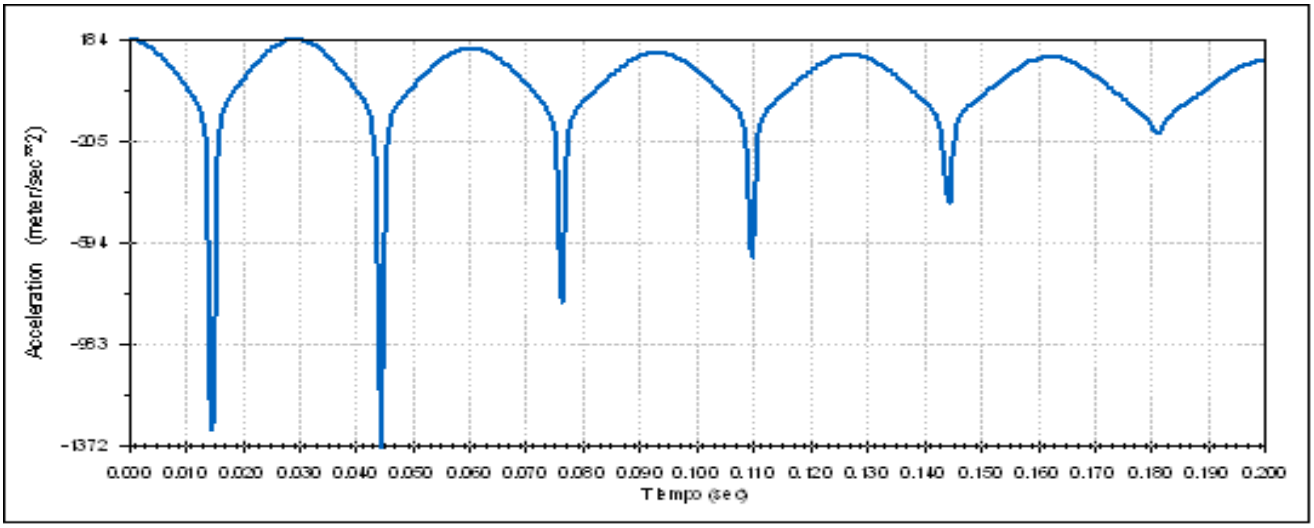

Figure 38 Model1 - Acceleration in y of the Midpoint of the Coupler Link

6.2.3 DETERMINATION OF ACCELERATIONS FOR MODEL2

The accelerations in x and y of the coupler link were determined with the implementation of the motion study tool in SolidWorks. The graph 39 shows the accelerations in x.

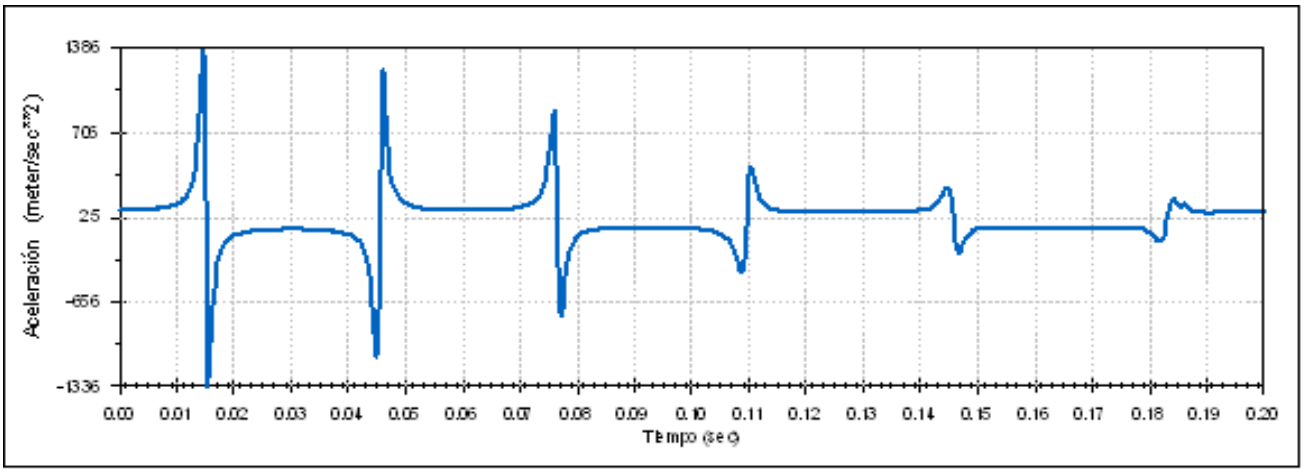

Figure 39 Model 2 - Acceleration in x of the Midpoint of the Coupler Link

The accelerations in y are given by figure 40

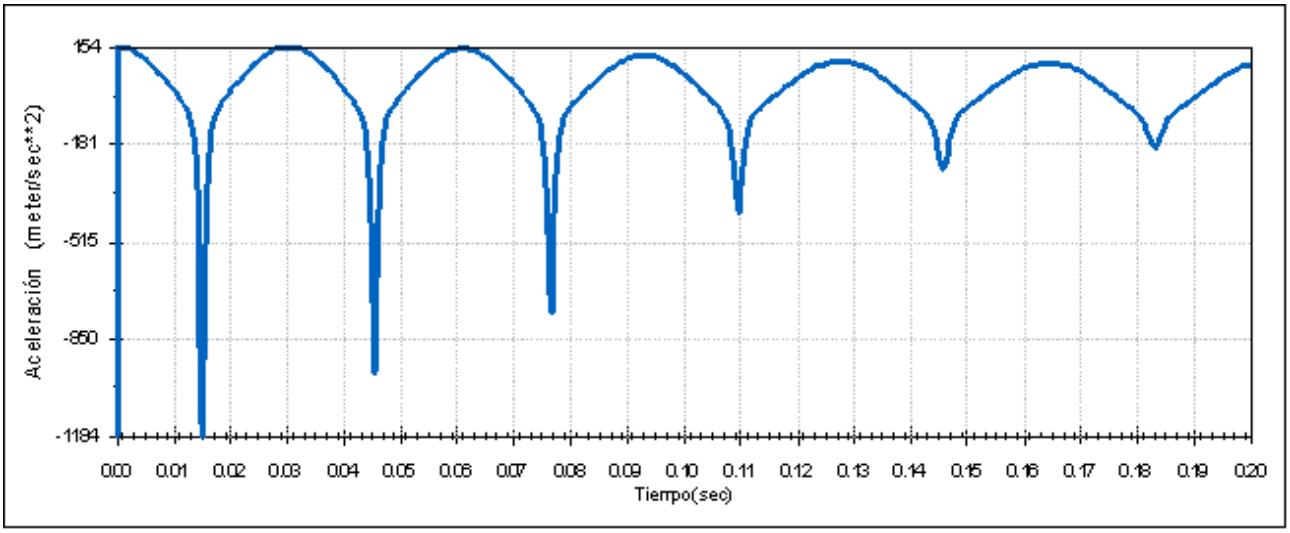

Figure 40 Model 2 - Acceleration in y of the Midpoint of the Coupler Link

6.2.4 DETERMINATION OF ACCELERATIONS FOR MODEL 3

The accelerations in x and y in the coupler link were determined with the implementation of the motion study tool in Solid Works. The graph 41 shows the acceleration in x.

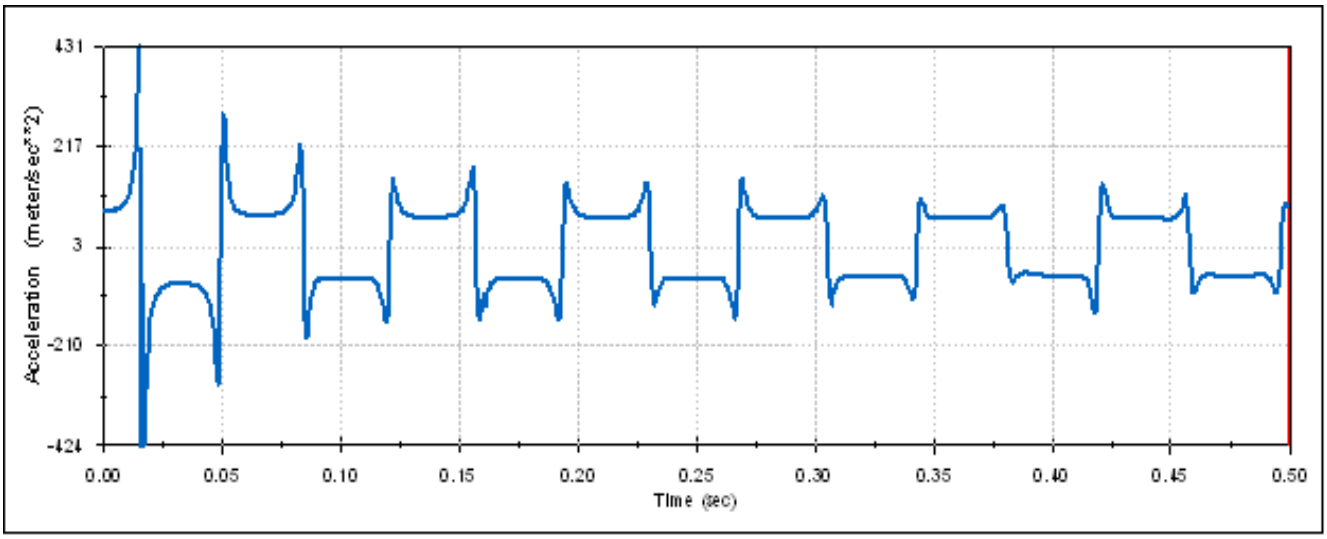

Figure 41 Model 3 - Acceleration in x of the Midpoint of the Coupler Link

The acceleration in y is given by figure 42.

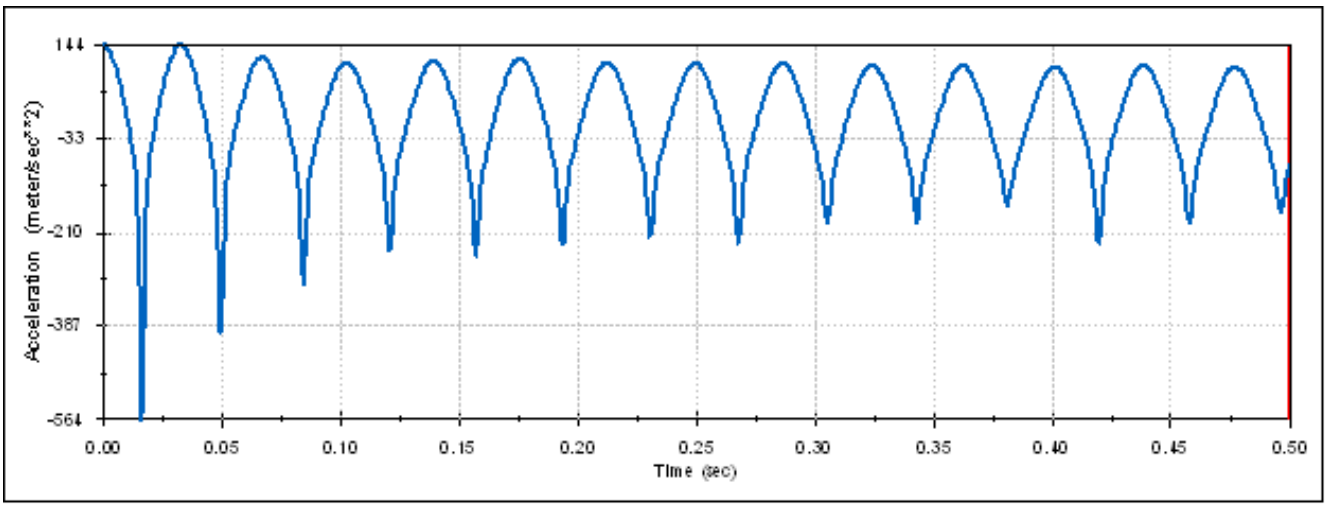

Figure 42 Model 3 - Acceleration in y of the Midpoint of the Coupler Link

6.2.5 TRANSIENT ANALYSES IN ANSYS™

Transient analyses were developed in ANSYS™ to analyze the different behaviors among the models. The displacements in x are described by figures 43, 44, 45 and 46:

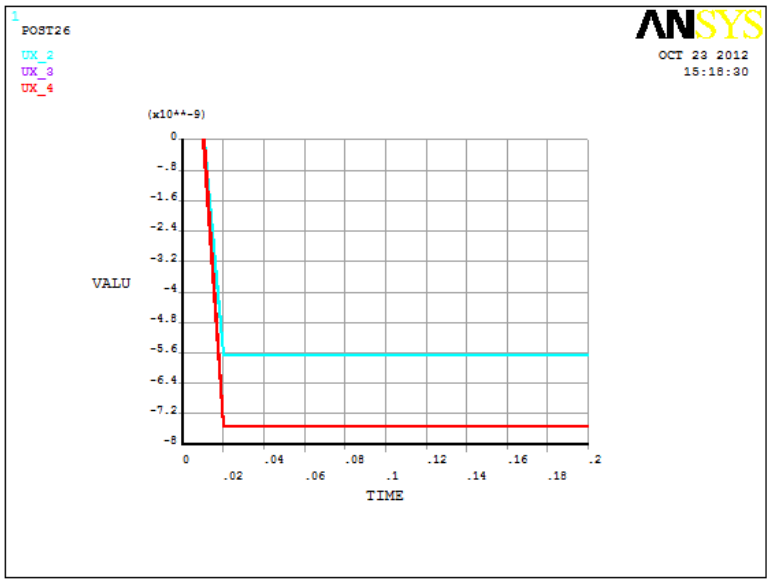

Figure 43 Model 0 Displacement in x

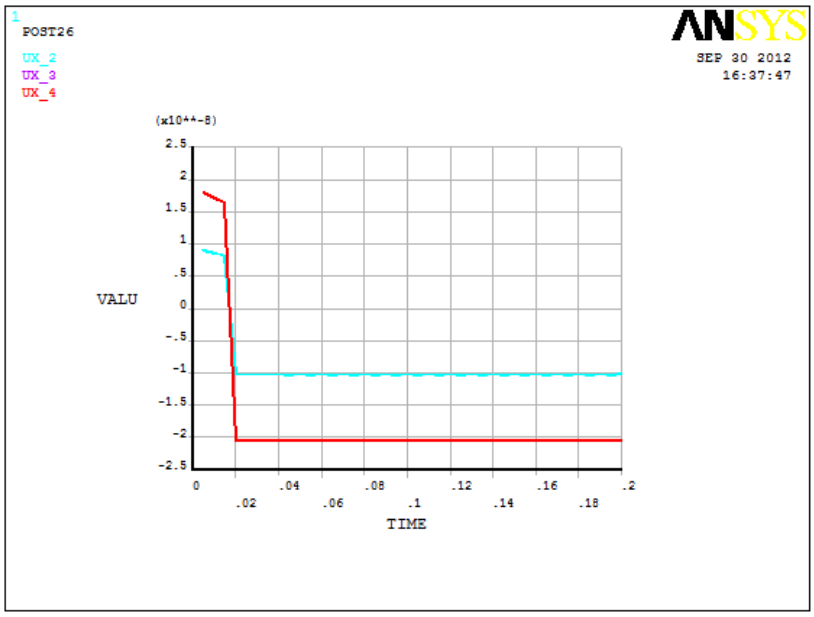

Figure 44 Model 1 - Displacement in x

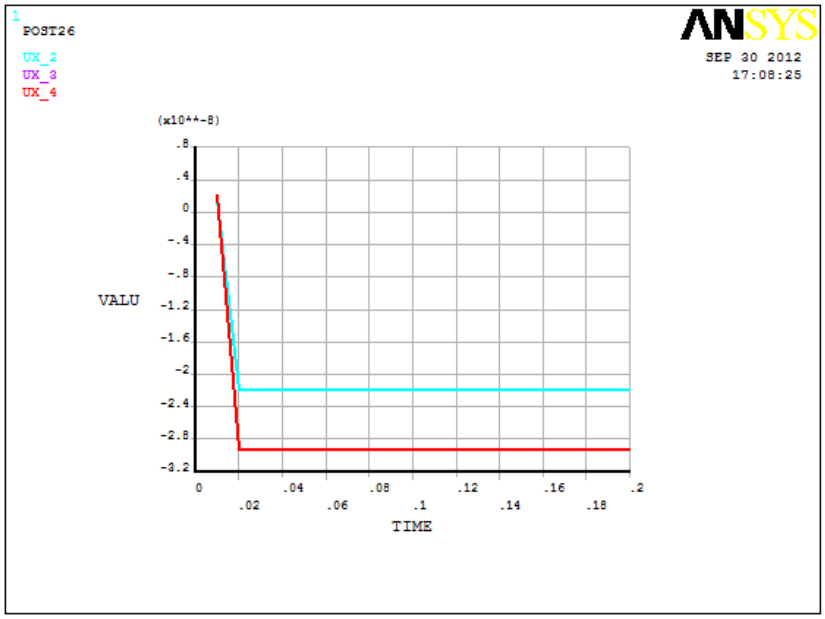

Figure 45 Model 2 - Displacement in x

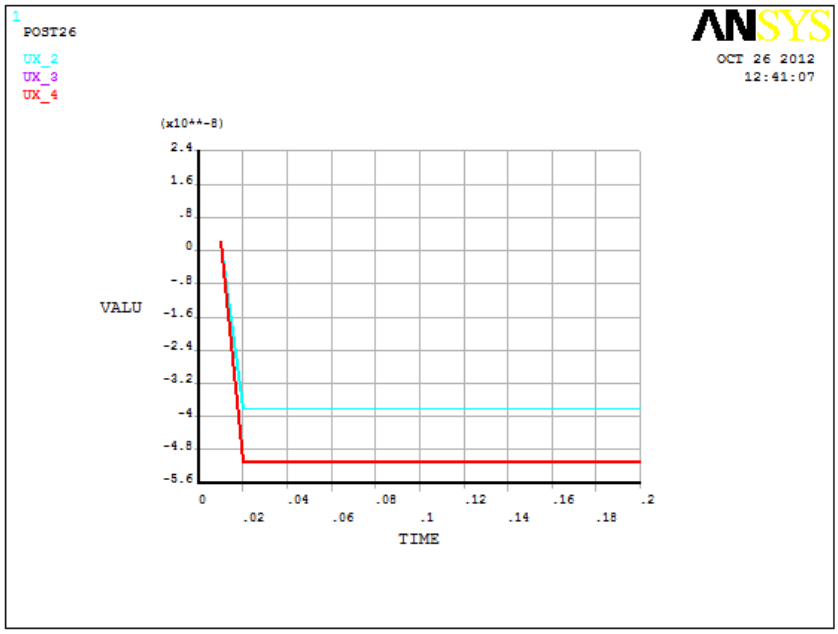

Figure 46 Model 3 - Displacement in x

The displacements in y are showed in the graphs 47, 48, 49 and 50.

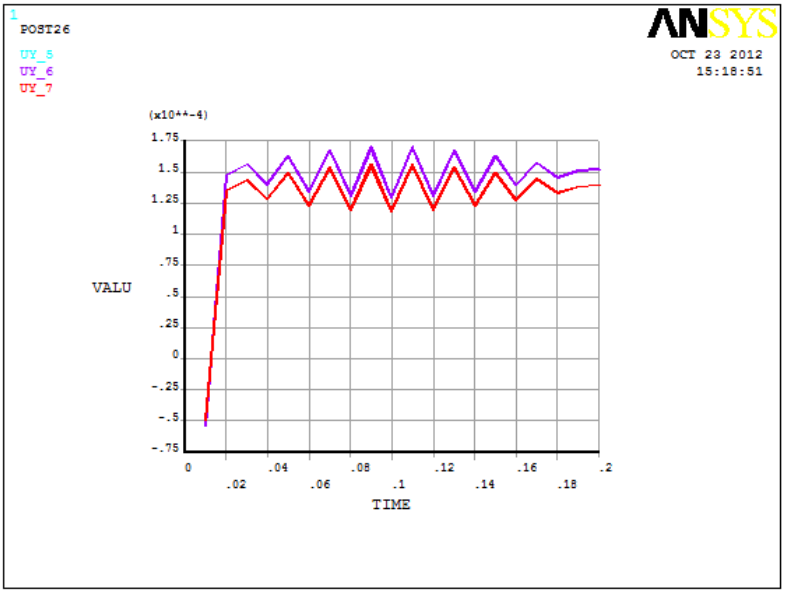

Figure 47 Model 0 - Displacement in y

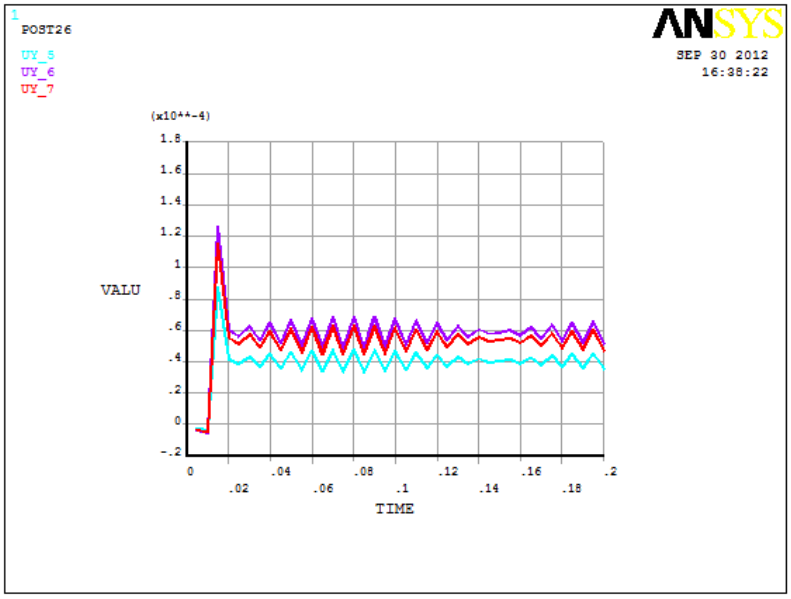

Figure 48 Model 1 - Displacement in y

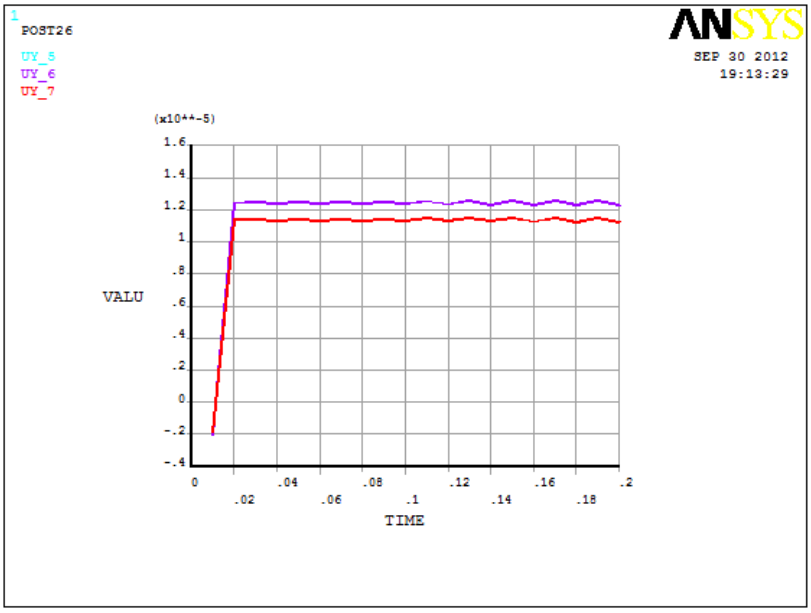

Figure 49 Model 2 - Displacement in y

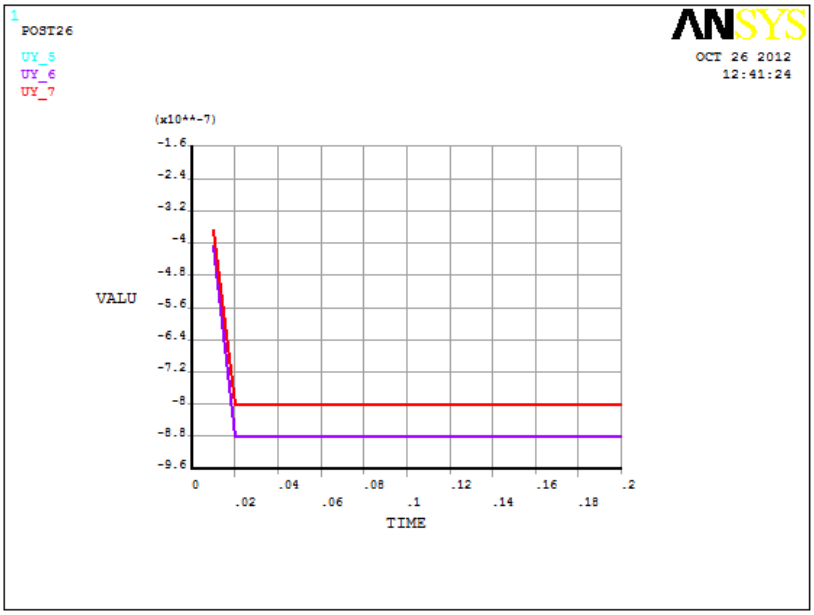

Figure 50 Model 3 - Displacement in y

The results obtained from the modal and transient analyses were compared with the deployment time of the mechanism. The objective of this comparison is to determine if the periods of the links are less, equal or greater than the deployment time of the mechanism. This comparison allows determining if the bodies can be considered as rigid or flexible bodies. If the period of the link (T) is greater than the deployment time (Δt) , the bodies can be considered as a flexible.

$$kT > \Delta t \qquad \text{Eq. 64}$$

The assumption of rigid body can be adopted if the period of the link multiplied by k is less than the deployment time.

$$kT < \Delta t \qquad \text{Eq. 65}$$

k is the times that the natural period is less that the deployment time.

By comparing the graphs obtaining above in the transient and modal analyses and the information on table 5, it is possible to define the parameter k. Consequently, the k value can be defined as a 108.

6.3 MODAL ANALYSES OF THE CRANK AND COUPLER LINKS IN THE HIGH SPEED DEPLOYMENT SLIDER – CRANK.

Modal analyses were performed in the commercial software ANSYS ^{TM} to study the behavior of the crank and the coupler link. The links were analyzed by separately and each link was modeled as a beam. A modal analysis was run to obtain the frequency of the crank and the coupler link. Finally, the period can be calculated from the result of ANSYS ^{TM} and the assumption of rigid body in this model can be verify.

6.2.1 MODAL ANALYSIS OF THE CRANK IN ANSYS

The crank was modeled in ANSYS as a beam and 5 modes were analyzed. The element type which was used is beam 2 node 188. The material properties as shown in the table 7:

Material	Steel ASTM - A36
Modulus of elasticity	200 000 000 000Pa
Density	7850.00 kg/m^3

Table 6 Material Properties

The result for the modal analysis of the crank are given in the following table

SET	TIME/ FREQ	LOAD STEP	SUBSTEP	PERIOD (T)
1	13254	1	1	0.000075
2	24536	1	2	0.000040
3	31598	1	3	0.000031
4	36431	1	4	0.000027
5	45426	1	5	0.000022

Table 7 Modal Results

The mode 1 is shown in the figure 51:

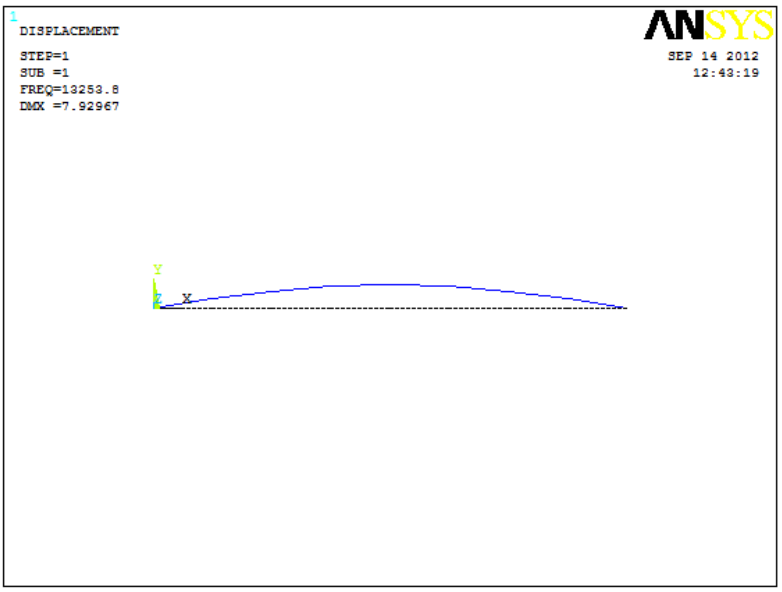

Figure 51 Mode 1 Crank link

Mode 4 is described in the figure 52.

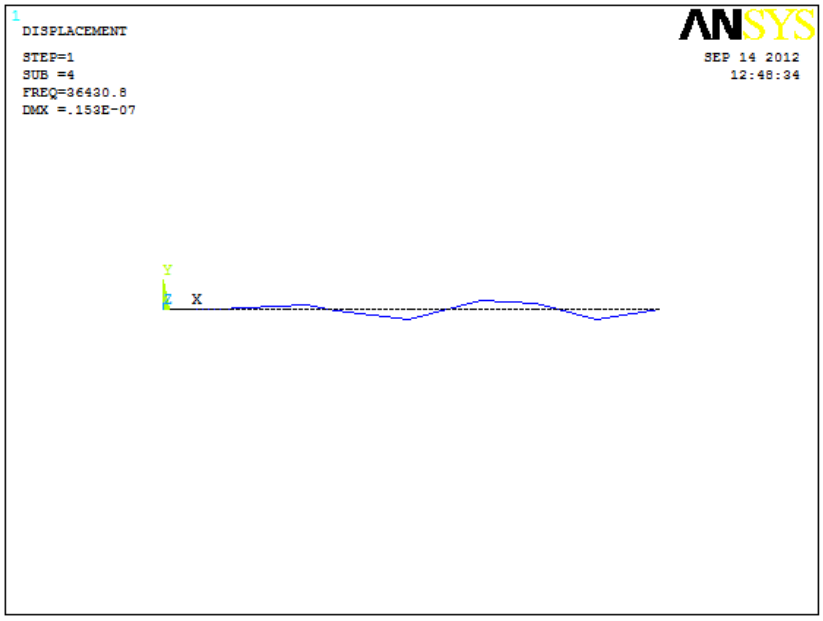

Figure 52 Mode 4 Crank Link

Mode 5 is shown in the figure 53

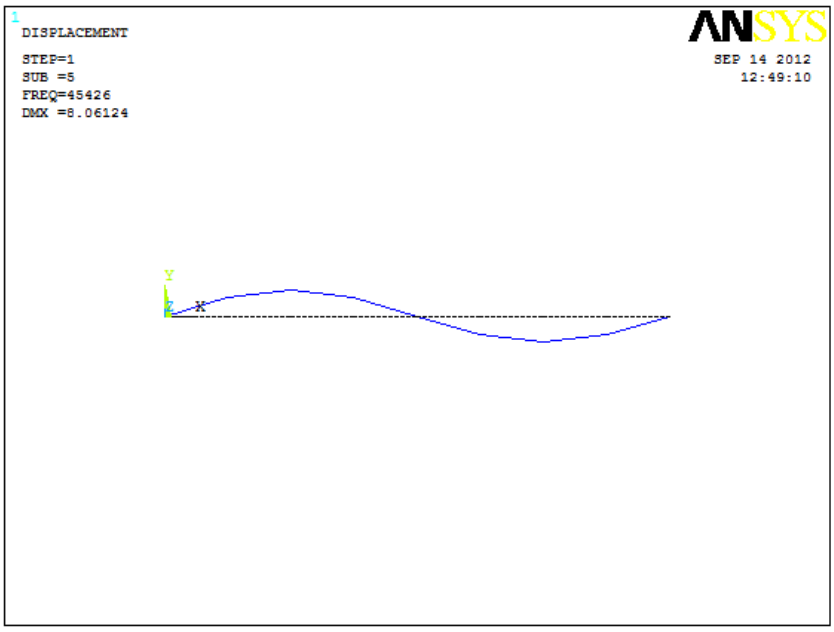

Figure 53 Mode 5 Crank Link

6.2.2 MODAL ANALYSIS OF THE COUPLER LINK IN ANSYS

The crank was modeled in ANSYS as a beam and five modes were analyzed. The element type which was used is beam 2 node 188. The material properties as shown in the following table:

Material	Steel ASTM - A36
Modulus of elasticity	200 000 000 000Pa
Density	7850.00 kg/m^3

Table 8 Material Properties

The result for the modal analysis of the coupler are given in the following table

SET	TIME/ FREQ	LOAD STEP	SUBSTEP	PERIOD (T)
1	3548.4	1	1	0.000281
2	7631.5	1	2	0.000131
3	13922	1	3	0.000071
4	15799	1	4	0.000063
5	18215	1	5	0.000054

Table 9 Modal Results

The mode 1 is shown in the figure 54:

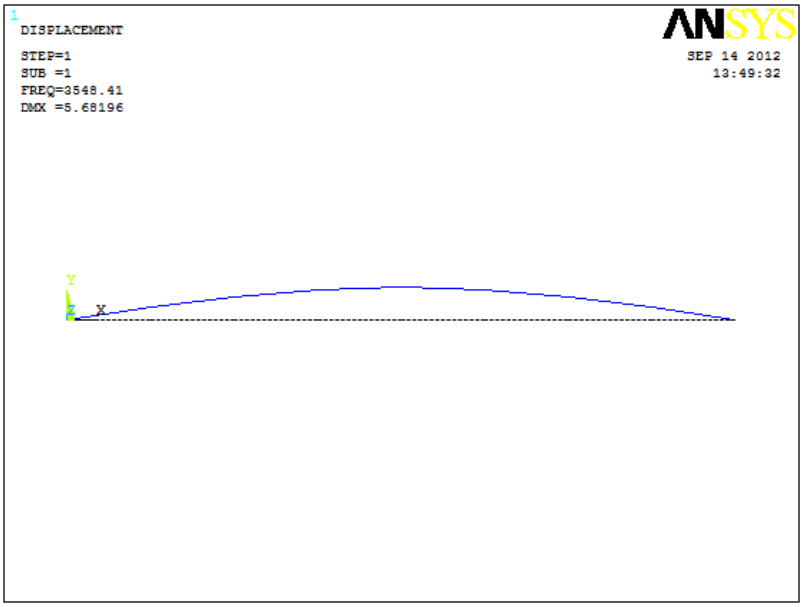

Figure 54 Mode 1 Coupler Link

Mode 5 is shown in the figure 55

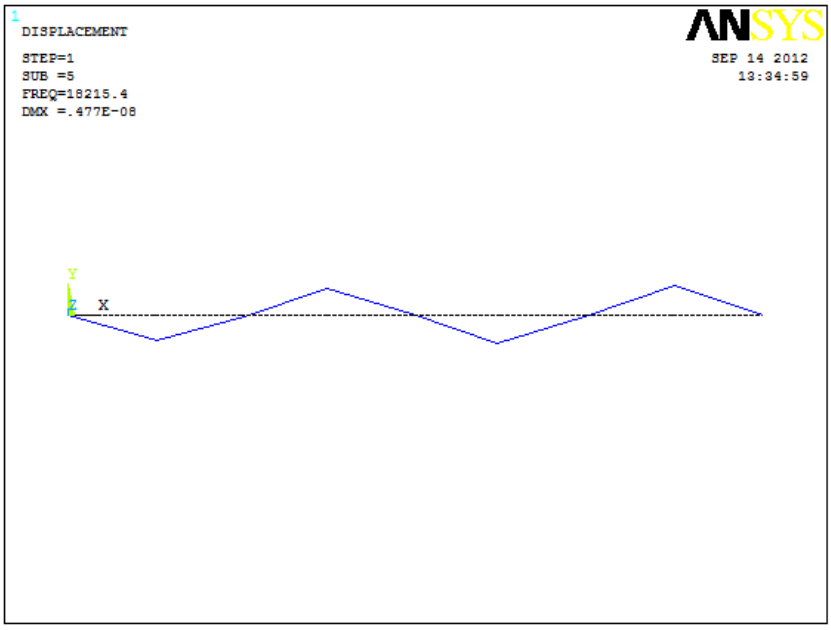

Figure 55 Mode 5 Coupler Link

The crank and coupler link of the slider crank showed in figure 1 behave as rigid bodies and it can be verified from the Eq. 65

For the crank link

$$T\,(0.000022) < \Delta t\,(0.016128) \qquad \text{Eq. 66}$$

From Eq. 66 the value of k can be calculated:

$$k = 733$$

Therefore, the crank link can be considered as a rigid body.

For the coupler link

$$T(0.000054) < \Delta t\,(0.016128) \qquad \text{Eq. 67}$$

From Eq. 67 the value of k can be calculated:

$$k = 299$$

Therefore, the assumption of rigid body in the coupler link can be adopted.

6.4 AEROSPACE ILLUSTRATIVE APPLICATION OF A HSDM

High Speed Deployment Mechanisms have a wide range of applications such as aerospace, cryogenic, ballistic and industrial applications. The dynamic and kinematic analyses of those mechanisms are essential for a high performance and a high reliability of systems. In addition, design considerations, complementary calculations and further analyzes need to be addressed in the design scenario.

This section presents an illustrative aerospace application of the mechanism analyzed in chapters 4, 5 and 6. The slider crank mechanism is implemented in a missile which has high speed deployment wings. The wings are deployed after the missile is launched. The figure 56 shows the missile analyzed:

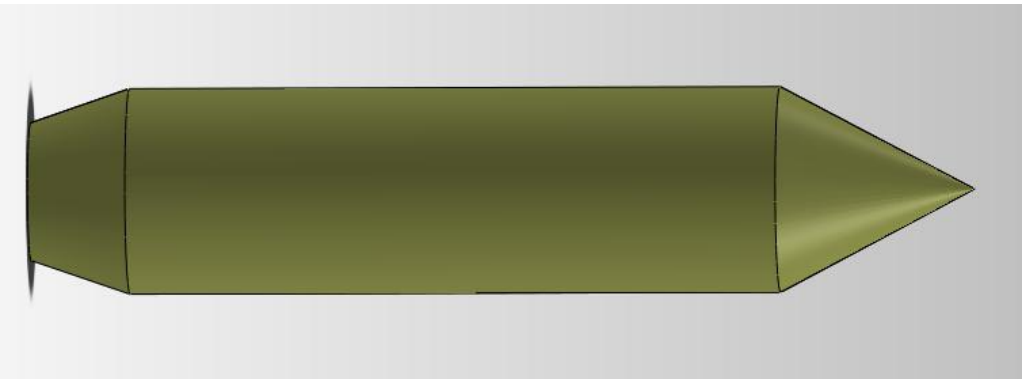

Figure 56 Missile

The mechanism of the wings in the initial position is shown in figure 57

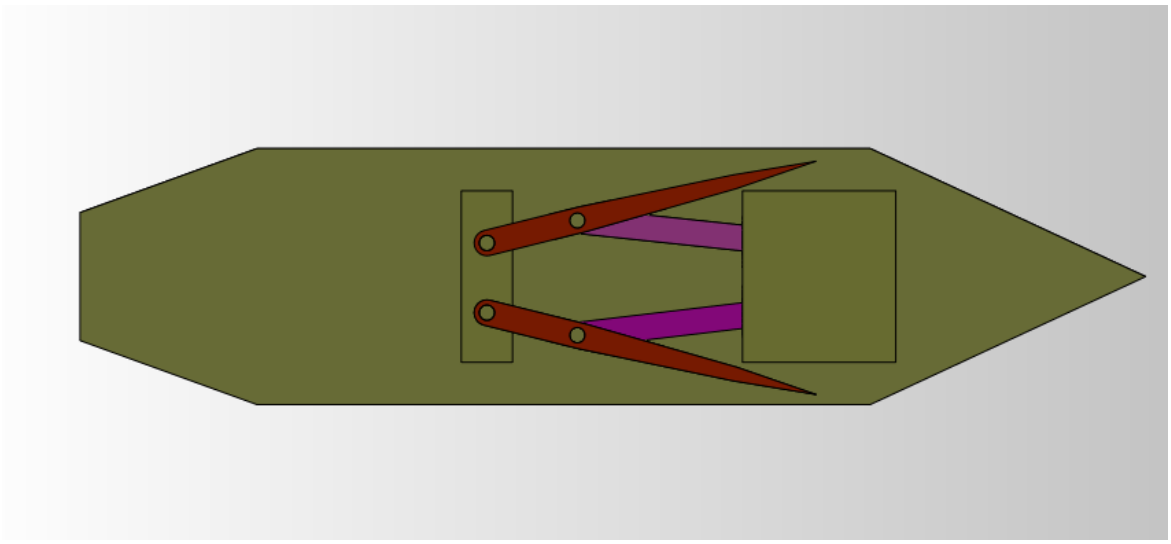

Figure 57 Initial Position of the Wing's Mechanism

The final position of the mechanism is presented in figure 58

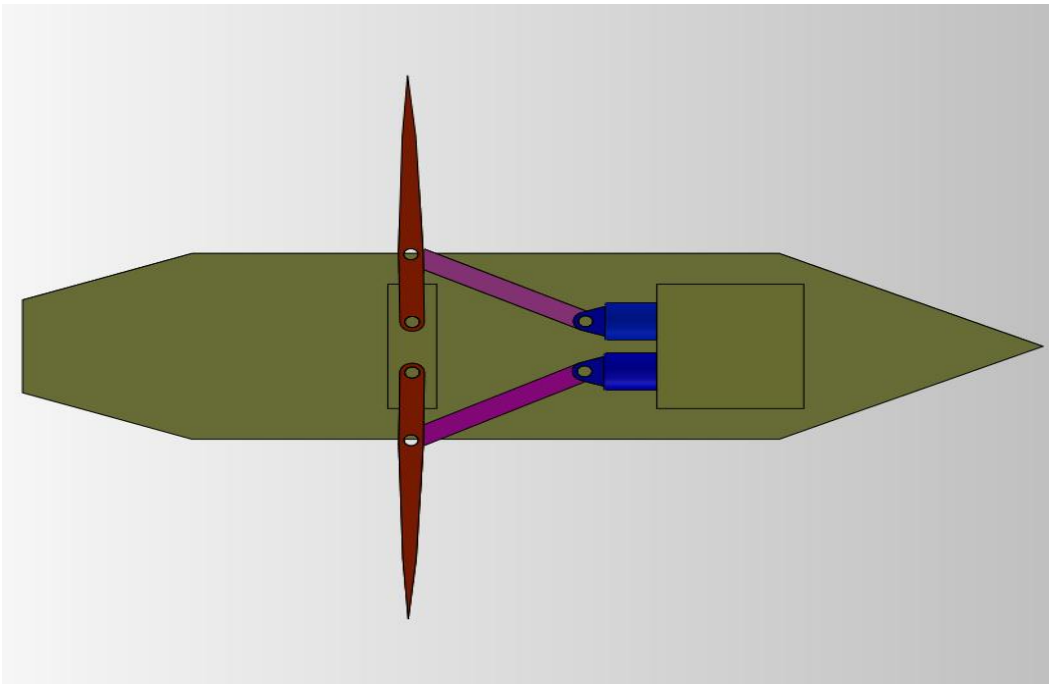

Figure 58 Final Position of the Mechanism

The deployment time from the original position to the final position is approx. 0.017 s.

The angular displacement of the tip of a wing is shown in the figure 59:

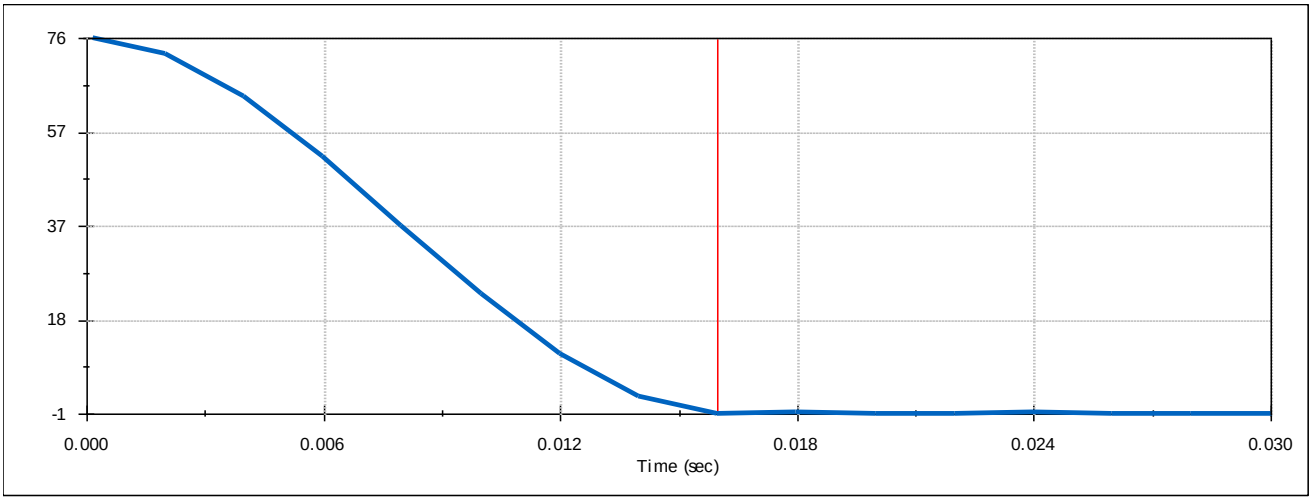

Figure 59 Angular Displacement

The angular velocity of the tip of the wing is given by figure 60:

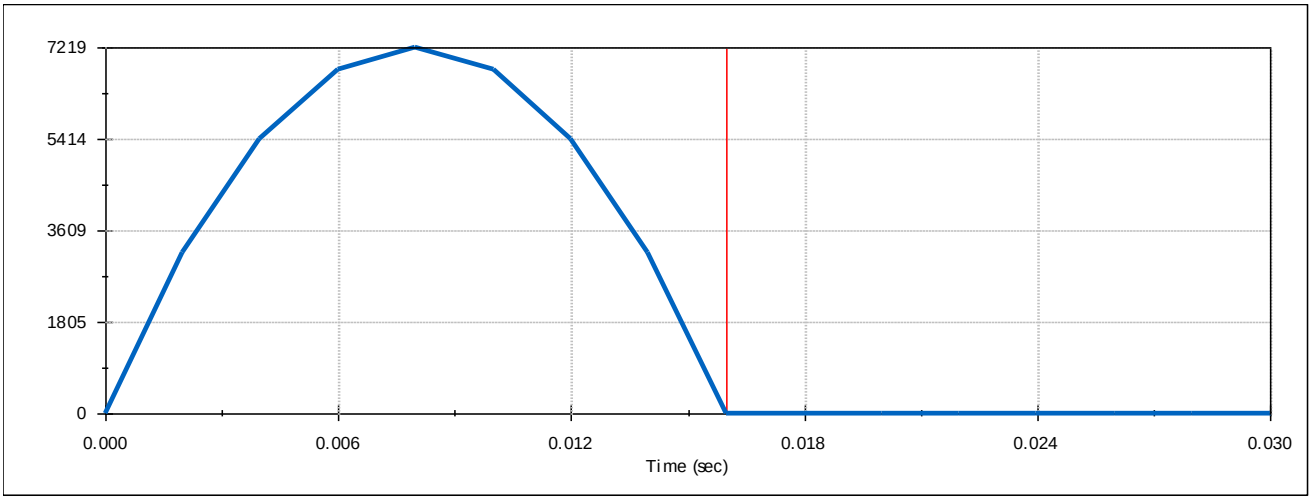

Figure 60 Angular Velocity

The maximum angular velocity is reached at .008 s (approx.) with a value of 7219 deg/sec.

CONCLUSION AND FUTURE WORK

The purpose of this research was to present a systematic approach to analyze a Slider-Crank Deployment Mechanism. The methodology presented in the previous chapters establishes a reference frame in the literature to study the flexibility and transient dynamic response of a Slider-Crank Deployment Mechanism. Furthermore, this methodology was based on established mathematical models and theories developed by well-known mathematicians and scientists such as Lagrange, Kutzbach, Hamilton and more. The kinematic and dynamic analyses of the mechanism were performed satisfactorily and the results obtained in the calculations were reliable. In addition, some Finite Element simulations of the components were developed; the results from this research were validated with the implementation of commercial software. Moreover, an illustrative aerospace application of a High Speed slider –crank mechanism was presented. Finally, a criterion to establish the use of rigid or flexible body assumption in a Slider-Crank Deployment Mechanism was proposed.

The first part of this work, presented an approach to perform the kinematic and the dynamic analyses of a Slider – Crank mechanism. Those analyses were developed in a Multibody code in Matlab which was based on the Lagrange Multipliers method. This

code was also based on new techniques developed by the University of Rome Tor Vergata, Italy. Finally, the position, velocity, acceleration and reaction forces were obtained for kinematic and dynamic analyses. The results were validated with the implementation of commercial software such as ANSYS^{TM}, SOLIDWORKS^{TM}, ABAQUS^{TM} and MATLAB^{TM}.

This research also presented some considerations of design and finite element analyses of components of the mechanism. In addition, some modal analyses were carried out to determine the frequencies of the links. These results were used to propose a criterion which is based on the comparison of the natural period of the links and the time of deployment of the mechanism. This criterion has created a starting point in the literature in order to identify if the assumption of rigid body can be adopted in a Slider-Crank Deployment Mechanism

In summary, this research proposed two important contributions in the literature of HSDM: First, a methodology to address the kinematic and dynamic analyses of a Slider-Crank Deployment Mechanism. Second, a criterion to verify if the assumption of using rigid bodies in a Slider-Crank Deployment Mechanism can be adopted.

Future Work

The field of High Speed Deployment Mechanisms is still unexplored in many areas; the literature review showed that there are not many researches or publications about it. However, HSDM are becoming fundamental in specific applications. To name an example, the aerospace industry uses this type of mechanism for some applications. Consequently, the field of HSDM is a potential research area to develop new theories and techniques in order to emphasize the differences between Non High Speed Deployment Mechanisms and High Speed Deployment Mechanisms. Essential topics need to be addressed in this area such as i) Joint design for HSDM ii) Consequences of clearance, friction and contact in joints and elements in the design scenario iii) Classification of these type of mechanisms iv) How to differentiate High Speed Deployment Mechanisms from Non High Speed Deployment Mechanisms?.

REFERENCES

[1] SAROVAR, S., Significance of design context and rationale in long term retention of data. West Virginia (2009).

[2] NORTON, R. L., Design of machinery. Third edition (2004). Mc Graw Hill.

[3] PANKOW, D., BESUNER, R., WILKES, R., and ULLRICH, R., Deployment mechanisms on the fast satellite.

[4] ROSSONI, P., COOPERRIDER, C. and DURBACK, G. Deployment mechanism for the space technology 5 micro satellite.

[5] KERHOUSSE, P. and SICRE, J. Deployment mechanism for stentor deployable radiator. European space agency (1997), pp. 83-87.

[6] WALLRAPP, O., and WIEDEMANN, S. Simulation od deployment of a flexible solar array. Multibody System Dynamics(1998), pp. 1-24.

[7] STROM, S., KRABBEROD J. and CONDAMINET O. Design and development of the nozzle deployment mechanism for the Vinci Cryogenic Engine.

[8] NARAYANA, B., NAGARAJ, B.P., and NATARAJU, B.S. Simulation of deployable Polyhedral Truss. 13th National conference on mechanisms and machines (2007). Bangalore, India.

[9] OSMAN, M.O.M. and DUKKIPATI R.V. Velocity fluctuation in spatial four link mechanisms. Journal of Mechanical Engineering Science (1981), pp. 143-147.

[10] RANJBARKOHAN, M., RASEKH M., HOSEINI, A. H., KHEIRALIPOUR, K., and ASADI, M.R. Kinematic and kinetic analysis of the slider crank mechanism in otto linear four cylinder Z24 engine. Journal of mechanical engineering research (2011) Vol. 3(3), pp. 85-95.

[11] FLORES, FERNANDEZ, J. P. Dynamic analysis of mechanical systems with imperfect kinematic joints (2004).

[12] KOSHY, C.S. Characterization of mechanical systems with real joints and flexible links (2006).

[13] CONDON, J.A., and HOLLIS, M. S. L. Dynamic analyses of the mortar dragster tab mechanism. Army research laboratory (1998).

[14] BAUCHAU, O. A. and RODRIGUEZ, J. Modeling of joints with clearance in flexible multibody systems. International journal of solid and structures (2002), pp. 41-63.

[15] SHWAD, A.L., MEIJAARD, J.P., and MEIJERS, P. A comparision of revolute joint clearance models in the dynamic analysis of rigid and elastic mechanical systems. Mechanism and machine theory (2002).

[16] RAMAN, C.V. Some applications of Hertz's theory of impact. Vol. XV No. 4. 277-284.

[17] FU, G. An extension of Hertz's theory in contact mechanics. Journal of applied mechanics (2007) pp. 373-374.

[18] EARLES, S. W. E., and SENEVIRATNE, L. D. Design guidelines for predicting contact loss in revolute joints of planar linkage mechanisms (1990), pp. 9-18.

[19] HAMILTON, G. M. Explicit equations for the stresses beneath a sliding spherical contact. ImechE (1983). pp. 53-59.

[20] BOOKER, J. F., Squeeze films and bearing dynamics (1983). Vol. II. pp. 121-137.

[21] LEE, K. H., KIM, J. W., HUH, Y. J., and LEE, J. Optimum design of dynamically – loaded journal bearing with R600a refrigerant application (1998).International compressor engineering conference. pp. 153-158.

[22] DOWSON, D., FISHER, J., JIN, Z. M., AUGER, D. D., and JOBBINS, B. Design considerations for cushion form bearings in artificial hip joints (1991). pp. 59- 68.

[23] MA, Z. D., WANG, H., and RAJU, B. Function – oriented material design of joints for advanced armors under ballistic applications (2004). pp.1- 8.

[24] NAKALSWAMY, K. K., Experimental and numerical analysis of structures with bolted joints subjected to impact loads (2010).

[25] SANGREE, J., MARSH, J., MACDONAL, K., GAUTHIER, J., JONES, S., and MIKESKA, J. Nanosatellite separation experiment using a p-pod deployment mechanism. pp. 1 - 34.

[26] SAPNA, G. H., FOLKE, J., SANDY, C. R. and CADOGAN, D. P. Inflatable boom controlled deployment mechanism for inflatable sunshield in space (ISIS) flight experiment. 34th Aerospace mechanisms conference (2000).

[27] OLIVER, R., FALCKE, H. Creation of the deployment mechanism of an antenna. Radboud Universiteit Nijmegen (2010).

[28] MURATA, Y., HIRABAYASHI, H., NATORI, M. C., UMEMOTO, T., ASADA, K., IIKURA, S., and The next generation space VLBI working group. Development of the large and high accuracy deployable antenna for the VSOP -2 mission.

[29] HAROUN, A. F., and MEGAHED, S.M. Simulation and experimentation of multibody mechanical systems with clearance revolute joints. World academy of science, engineering and technology (2012). pp. 680-689.

[30] CHELI, F. and PENNESTRI, E. Cinematica e dinamica dei sistemi multibody. Casa Editrice Ambrosiana. Vol. 1 2006.

[31] SHABANA, A. A. Computational dynamics. A wiley – interscience publication. Second edition (2001).

[32] MARITI LORENZO, MUCINO VICTOR H., PENNESTRI ETTORE, CAVEZZA ANDRES, VALENTINI PIER PAOLO and MRIDUL GAUTAM. Optimization of a High Speed Deployment Slider Crank Mechanism: A Design Charts Approach (2012).